Geoscience Frontiers 7 (2016) 359–374

HOSTED BY

ELSEVIER

Contents lists available at ScienceDirect

China University of Geosciences (Beijing)

Geoscience Frontiers

journal homepage: www.elsevier.com/locate/gsf

Research paper

The giant Kalgoorlie Gold Field revisited

Noreen Mary Vielreicher [a,*], David Ian Groves [b], Neal Jesse McNaughton [c]

[a] *Department of Material Science and Physics, University of Salzburg, Hellbrunnerstrasse 34, 5020 Salzburg, Austria*
[b] *Centre for Exploration Targeting, University of Western Australia, 35 Stirling Highway, Crawley 6009, Western Australia, Australia*
[c] *John de Laeter Centre for Isotope Research, Curtin University, Kent St, Bentley 6845, Western Australia, Australia*

A R T I C L E I N F O

Article history:
Received 24 June 2015
Received in revised form
31 July 2015
Accepted 31 July 2015
Available online 19 August 2015

Keywords:
Kalgoorlie
Golden Mile
Mount Charlotte
Gold giant
Orogenic gold
Magmatic-hydrothermal gold

A B S T R A C T

The Neoarchaean Kalgoorlie Gold Field contains the giant Golden Mile and world-class Mt Charlotte deposits, which have been the subject of much research for over 100 years. The Golden Mile deposit is a complex array of ductile to brittle vein and breccia lodes that are predominantly hosted in the highly-fractionated Golden Mile Dolerite sill. The Fimiston lodes comprise an array of narrow lodes that evolved broadly syn- to late-formation of the regional D2 NW-trending foliation. The lodes are characterized by pyrite veinlets and disseminations, quartz veinlets and breccias, and banded quartz-carbonate veins with sericite, carbonate, and pyrite-dominated alteration. Bonanza Green-Leader, or Oroya-style, lodes, with grades in excess of 1000 g/t Au, are similar to the Fimiston-style lodes, but are characterized by abundant visible gold, native tellurium and more abundant telluride minerals within roscoelite-bearing alteration zones. The arguably structurally younger Mt Charlotte-style lodes are characterized by a pipe-shaped, coarse-grained quartz, carbonate and scheelite vein-stockwork with distinct vertically-zoned, carbonate-sericite-albite-pyrite ± pyrrhotite dominant alteration assemblages around veins within Unit 8 of the Golden Mile dolerite and porphyry dykes. The network of steep- and gently-dipping extension and shear fracture-fill veins are associated with NE-trending fault sets that cross cut the regional NW-trend. The deposit area is intruded by swarms of porphyry dykes, including syn-volcanic mafic dykes, early and volumetrically most significant c. 2.67 Ga feldspar-phyric porphyry dykes, as well as later c. 2.66–2.65 Ga calc-alkaline hornblende-phyric dykes associated with younger c. 2.65–2.64 Ga lamprophyre dykes. All post-volcanic dykes have similar orientations to the Fimiston lodes. The feldspar dykes are clearly overprinted by all styles of mineralization, although the relationship between hornblende-phyric and lamprophyre dykes and gold mineralization is more ambiguous. Most agree that gold mineralization was post-peak regional metamorphism of host rocks, although its relative structural timing is controversial.

Direct timing constraints on gold mineralization indicate that Fimiston- and Mt Charlotte-style mineralization formed within a relative short period of time around 2.64 Ga, and, as such, support a model of progressive deformation of a rheologically heterogeneous rock package late in the structural history. Fluid characteristics, combined with the structural, metamorphic and absolute timing, support description of gold mineralization at the Golden Mile as orogenic and mesozonal, and this allows direct correlation with orogenic gold deposits worldwide, which classically formed during accretion along convergent margins throughout Earth history.

1. Introduction

The Kalgoorlie Gold Field lies approximately in the centre of the well-endowed, Neoarchaean, Kalgoorlie granite-greenstone Terrane in the eastern Goldfields Province of the Yilgarn Craton in Western Australia (Fig. 1). The Gold Field is centered in and around the Golden Mile dolerite and is characterized by two dominant ore types: the mostly ductile style-Fimiston and brittle-style Mt Charlotte lodes. The majority of gold is produced via two mining operations. In the southeast, the remains of over 1000 named ore lodes, hosted within the shear zone system of the giant Golden Mile, are mined via the Fimiston open pit; a superpit measuring over 3.5 km

* Corresponding author.
E-mail address: noreenmary.vielreicher@sbg.ac.at (N.M. Vielreicher).
Peer-review under responsibility of China University of Geosciences (Beijing).

http://dx.doi.org/10.1016/j.gsf.2015.07.006

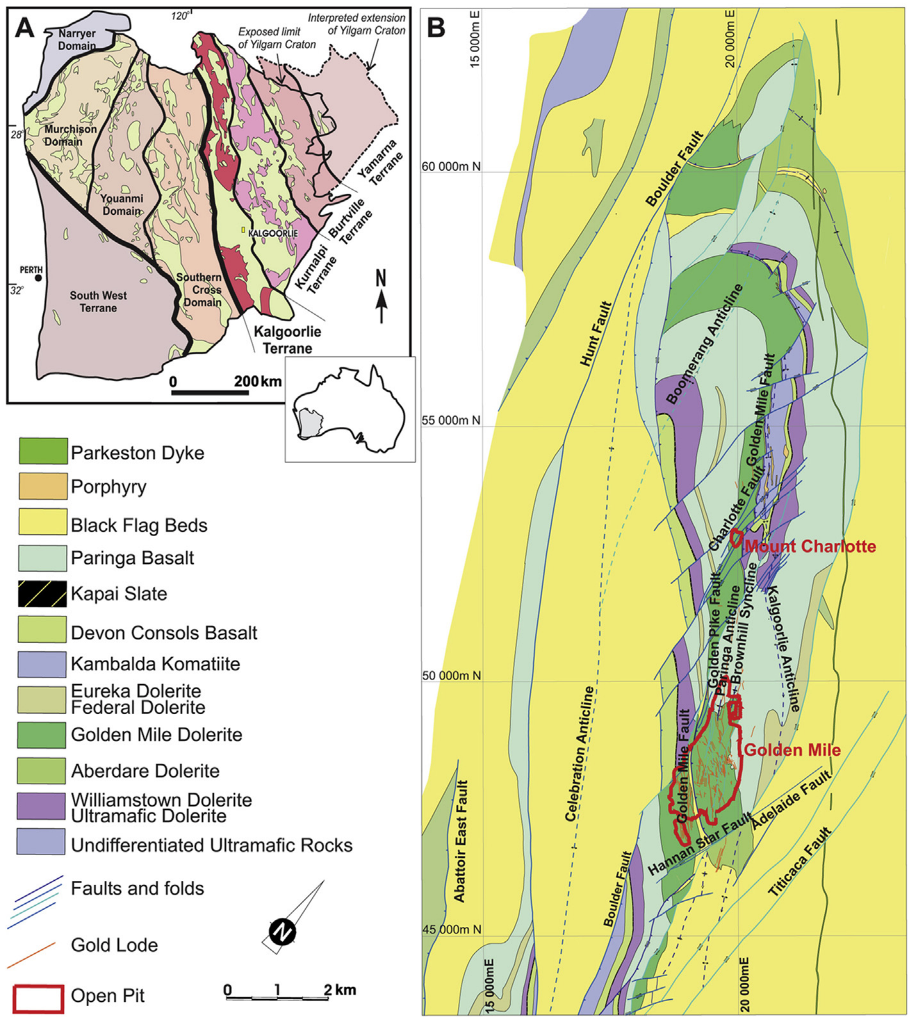

Figure 1. Location and geology of the Kalgoorlie area. (A) Yilgarn Craton as a mosaic of amalgamated gneiss, granitoid (both shown in shades of red depending on Terrane/Domain) and greenstone (green) bearing Terranes and Domains. Yellow coloured rectangle indicates location of the town of Kalgoorlie and Fig. 1B. Inset shows location of the Yilgarn Craton in Australia. (B) Geological map of the Kalgoorlie Gold Field showing major structures, the Golden Mile and Mt Charlotte mines and distribution of gold lodes. After Vielreicher et al. (2010).

long, >1.5 km wide and >500 m deep. In the northwest of the Gold Field, four orebodies (Reward, Charlotte, Maritana and Charlotte Deeps), consisting of predominantly brittle-style vein stockworks of the Mt Charlotte deposit, extend for about 1000 m along strike, approximately 1100 m vertically, and up to 90 m laterally, and are mined via underground bulk-mining, open-stope methods.

Gold has been continuously produced since June 1893, when three Irish prospectors, Dan Shea, Tom Flanagan and Paddy Hannan made the first discovery of gold in surface samples of quartz in the north of the Gold Field, near the current Mt Charlotte mine. After Paddy Hannan lodged the claim on 17 August, 1893, a gold rush ensued and the Golden Mile was discovered and exploited. Production in the Gold Field peaked in 1903 with 38.124 t (1,225,700 oz) of ore at an average grade of 41.1 g/t (1.32 oz/t) mined from predominantly gold-telluride lodes (Blainey, 1993). However, rising mining costs as lodes were followed underground and ores became more refractory, together with fixing of the gold price, led to a gradual drop in production. Nevertheless, by 1910, the Gold Field was well established with ten major shafts and numerous other smaller operations. Continued rising inflation associated with, and following, World War 1 kept mining activity at a low, but a re-evaluation of gold in the early 1930s led to a major revival. Production declined again in the 1960s, leading to cessation of mining on the Golden Mile in 1975. Production from the Mt Charlotte mine continued, however, due to the low-cost mechanized mining methods. The marked rise in gold price in 1975 sparked resurgence in mining, and the Golden Mile operations progressively reopened with new open-cut mines developed. Throughout its history, the mining operations in the Kalgoorlie Gold Field had been progressively consolidated into fewer and larger companies until 1989, when Alan Bond acquired and consolidated the final three companies into one operation that is now managed by Kalgoorlie Consolidated Gold Mines (jointly owned by Newmont and Barrick). The numerous lodes of the Golden Mile are currently mined via the Fimiston Superpit and, together with the Mt Charlotte underground mine, produce up to 850,000 ounces of gold each year. A total of 1670 t (351 Mt at 5.5 g/t Au head grade) and 144 t Au (42.6 Mt at 3.8 g/t Au) gold has been produced from the Golden Mile and Mt Charlotte, respectively, between 1893 and 2013. Gold deportment is approximately 30% native gold, 25% telluride gold, 35% gold inclusions in pyrite and 10% invisible inclusions in pyrite (Bateman et al., 2001). The refractory gold ore in pyrite and telluride minerals is roasted to liberate the gold.

The Gold Field has been continuously studied since gold was discovered, with the first mineralogical reports (e.g. Card, 1898; Frecheville, 1898), geological map (Maitland and Campbell, 1902) and structural evaluation (McLaren, 1910) produced just a few years after discovery. However, despite over a century of geological studies, controversy still reigns particularly with regard to the timing and genesis of gold mineralization. The current understanding of the gold deposits in the Gold Field is reviewed here to provide an overview of the current understanding of this giant ore system.

2. Tectonic and metallogenic setting of the Kalgoorlie Terrane

The majority of gold deposits in the many gold fields within the well-endowed Kalgoorlie Terrane, and those elsewhere in the Province, can be directly compared to other Neoarchean gold deposits around the world (e.g. in the Superior Province of Canada). The deposits are characterized by similar host-rock associations, potassic alteration, low sulphide- and telluride-bearing ore assemblages, a post-peak metamorphic timing in mostly greenschist-facies rocks, and gold grade and lode geometry that are strongly structurally controlled within lower-order structures adjacent to first-order crustal-scale faults (see summary in Robert et al., 2005).

The Kalgoorlie Terrane is one of several north-south elongated terranes (Fig. 1) that have been accreted to the continental margin of the Youanmi Terrane on the eastern edge of the Proto-Yilgarn craton in the Neoarchean (Fig. 2; Mole et al., 2013 and references therein). The rock sequences within the Kalgoorlie Terrane record both plume-related volcanism and volcanism that is consistent with an extensional back-arc setting behind a rifted mature arc (in the Gindalbie Domain; Barley et al., 1989, 2008; Krapež and Barley, 2008). The adjacent Kurnalpi Terrane to the east is defined by andesite-dominated volcanic complexes that were deposited in an intra-arc system (Barley et al., 1989, 2008; Krapež and Barley, 2008).

Two main models have been proposed for the tectonic setting during deposition and deformation of the arc-related, 2.72–2.69 Ga rocks of the Kalgoorlie and Kurnalpi Terranes: (1) a combination of both plume- and arc-related volcanism in an autochthonous rift developed above a westward-directed subduction zone that extended beneath the current Youanmi Terrane to the east, followed by closure and accretion of both terranes to the Proto-Yilgarn craton at 2.66–2.63 Ga (recent references by Czarnota et al., 2007, 2010; Blewett et al., 2010); (2) a pull-apart basin associated with strike-slip faulting and amalgamation of arc-related terranes, similar to the modern Philippines Archipelago (e.g. Barley et al., 2008; Krapež and Barley, 2008).

With respect to gold mineralization, geological evidence, together with precise geochronology, shows that deposits in the majority of gold fields in the Kalgoorlie Terrane formed during accretion of the Kalgoorlie Terrane to the Youanmi Terrane, prior to stabilization of the Yilgarn craton (e.g. Vielreicher et al., 2015). The deposits are therefore clearly orogenic in timing, but there is still dispute as to whether some are the result of orogenic or magmatic processes. Orogenic gold deposits typically form in Cordilleran-type accretionary zones, from a regional fluid type inherent to the prevailing tectonic processes (Goldfarb et al., 2005). There is much discussion as to the ultimate source of the fluid and the contained gold. The most common interpretations are that: (1) the fluid originated below mineralized supracrustal rocks in the

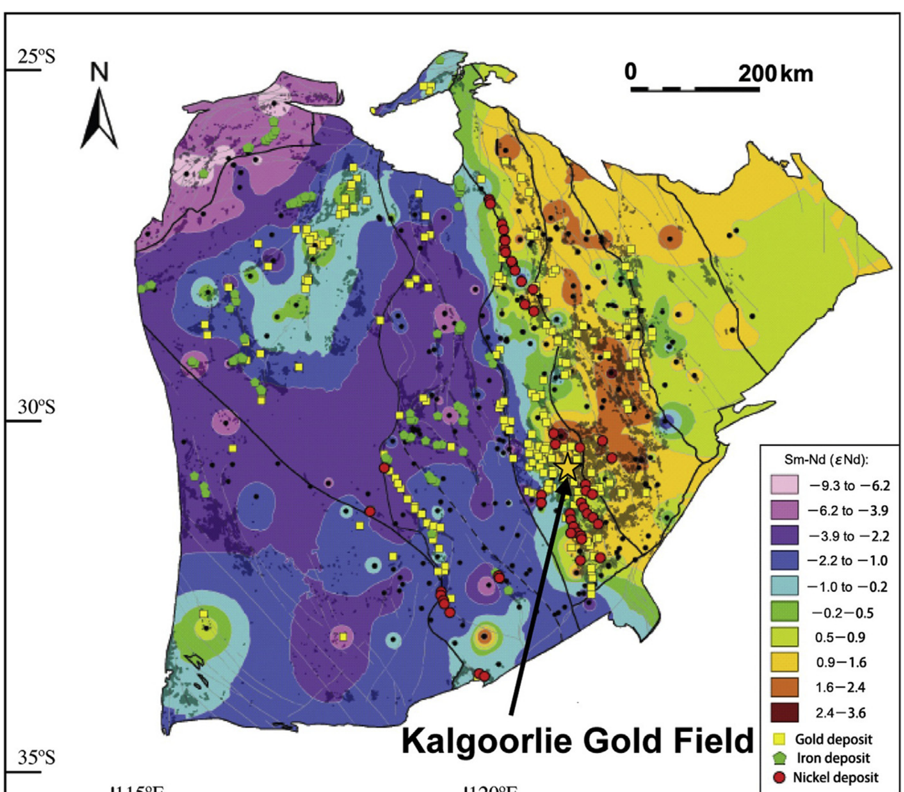

Figure 2. ε_{Nd} isotopic map of the Yilgarn craton at 2.7 to 2.6 Ga, showing distribution of ca. 2.7 Ga nickel deposits, ca. 2.65 Ga gold deposits, and BIF-hosted iron oxide deposits (after Mole et al., 2013; McCuaig and Hronsky, 2014). Note the location of the Kalgoorlie Gold Field along the strong N–NW-trending gradient in the centre of the craton, which is interpreted as representing the margin of the paleo-craton at ca. 2.7 Ga, with evolved crust to the west (the Proto-Yilgarn) and juvenile crust to the east (accreted terranes).

continental crust via metamorphic devolatilization (e.g., Phillips and Powell, 2009); or (2) from either devolatilization of the subducted slab, with overlying oceanic sediments, or the lithosphere below (e.g. Goldfarb and Santosh, 2014, based specifically on the Jiaodong province of China). Conversely, the proponents of magmatic-hydrothermal models invoke a direct local magmatic fluid and metal source that was related to spatially-related syenites or high Mg monzodiorite-tonalite intrusions (Robert, 2001; Mueller, 2015). Gold mineralization in the Kalgoorlie Gold Field is reviewed here, with particularly emphasis on its genesis and the controversy that surrounds it.

3. Geology of the Kalgoorlie Gold Field

The Kalgoorlie Gold Field is located within the Kalgoorlie Terrane (Fig. 1) that is bounded on the west by a lithospheric boundary, broadly marked by the regional east-dipping Ida Fault and to the east by the also east-dipping Mount Monger Fault (Swager, 1989). The terrane comprises a collage of six structural domains that contain metamorphosed, dismembered and thrust-repeated but correlatable 2.73–2.65 Ga rock sequences. These four unconformity-bound lithostraphic sequences include: the lowermost dominantly volcanic Kambalda Sequence, the Kalgoorlie Sequence of mostly volcaniclastic rocks, and the uppermost Kurrawang and Merougil Sequences of siliciclastic sedimentary rocks (Swager et al., 1992; Morris, 1993; Krapež, 1997; Krapež et al., 2000; Krapež and Hand, 2008).

The Kalgoorlie Gold Field is hosted within the Kambalda Domain, in an outlier of komatiites and basalts of the Kambalda Sequence, overlain by a >3000 m-thick succession of mostly dacitic, with lesser andesitic and rhyolitic volcaniclastic, sedimentary and volcanic rocks of the Black Flag Group (Woodall, 1965; Travis et al., 1971; Hunter, 1993; Hand, 1998; Krapež et al., 2000; Figs. 1 and 3). The Kambalda Sequence includes (from oldest to youngest) the

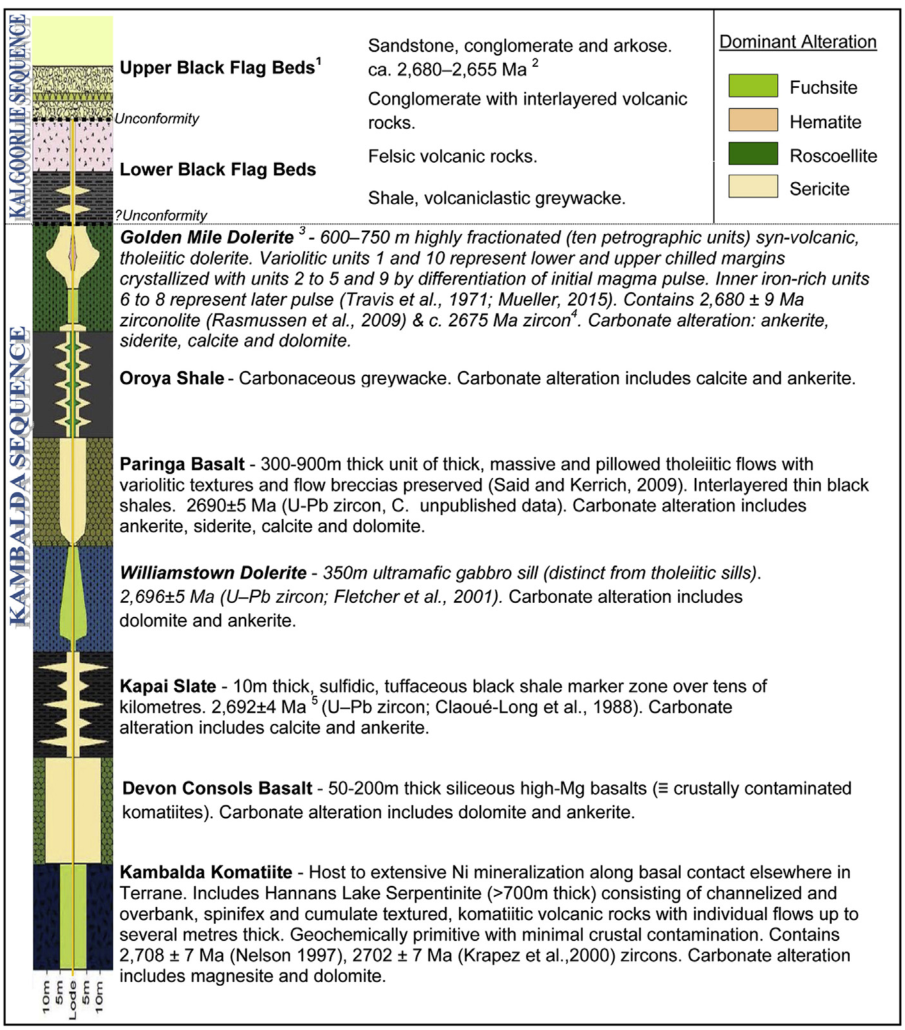

Figure 3. Host rock sequence to gold deposits at Kalgoorlie showing variation in dominant alteration mineral with lithology (after Nixon et al., 2014). Intrusive sills are described in italics. The basal unit of the Kambalda Sequence, the Lunnon Basalt (tholeiitic pillow basalts and flows), is not shown as it does not crop out in the Kalgoorlie area, although it is exposed further south at Kambalda. [1] The Upper Black Flag Beds are restricted to the southeast of the mining district, where conglomerates containing amphibolite and meta-andesite boulders overlie Golden Mile Dolerite on an erosional unconformity (Krapež and Hand, 2008). They host no known gold mineralization to date. [2] Based on detrital zircon ages of 2666 ± 6 Ma, 2669 ± 7 Ma, 2676 ± 5 Ma, 2679 ± 10 Ma, 2680 ± 5 Ma, 2681 ± 5 Ma, 2813 ± 3 Ma (Krapež et al., 2000 and references therein). [3] Subsurface geology at the Superpit suggests that there was ≥1 km of basalt above the Golden Mile Dolerite (Bateman et al., 2001). Interpreted emplacement depth for the Golden Mile Dolerite is ≥5 km: extra strata were removed prior to deposition of Upper Black Flag Beds (Krapež and Hand, 2008). [4] Based on 2673 ± 5 Ma (Claoue-Long et al., 1988), 2675 ± 2 Ma (Woods, 1997), 2675 ± 8 Ma (Heath, 2003) SHRIMP U-Pb zircon ages. NB Zircons are rimmed by zirconolite (Vielreicher et al., 2010). [5] Krapež et al. (2000) argued that the zircon age may be post-depositional.

Lunnon Basalt, Kambalda Komatiite, Devon Consols Basalt and Paringa Basalt with thin interlayered, in places tuffaceous, sedimentary units (Fig. 3; Swager et al., 1995; Nixon et al., 2014).

The Kambalda Sequence is unconformably overlain by four unconformity-bounded sequences of tonalite-trondhjemite-dacite (TTD) volcaniclastic and epiclastic rocks with subordinate rhyolite, dacite, andesite and tholeiitic basalt of the Kalgoorlie Sequence (Black Flag Group), and intruded by subvolcanic rhyolite and dacite sills and dykes, dolerite-gabbro sills and I-type granitoids that are spatially and temporally associated with the younger Kalgoorlie Sequence (Tables 1 and 2; Krapež and Hand, 2008). Based on regional field relationships and limited geochronology (Rasmussen et al., 2009) the differentiated, tholeiitic, Golden Mile Dolerite is generally considered to be an intrusive sill emplaced into carbonaceous greywacke along the upper contact of the Paringa Basalt, although Nixon et al. (2014) have recently revived speculation that it was part of the volcanic stratigraphy. Whatever its origin, it clearly played a particularly important role in the structural evolution of the district and is the main host to gold mineralization in the Kalgoorlie Gold Field (Fig. 1; Table 1). The rocks of the Kalgoorlie Sequence are interpreted to have been deposited in a series of transtensional deep-marine intra-arc basins (Hand, 1998; Brown et al., 2001; Krapež and Hand, 2008).

In addition to the synvolcanic c. 2.67 Ga rhyolite and dacite sills and dykes that are associated with the Kalgoorlie Sequence (Yeats et al., 1999; Gauthier et al., 2004; Vielreicher et al., 2010), there are also other high-level, subvolcanic, porphyry dykes (Table 2) including syn-volcanic mafic dykes and a 2.65 Ga fractionated suite of monzodiorite-granodiorite-tonalite, hornblende- to feldspar-phyric porphyry dykes (Mueller et al., 1988; Gauthier et al., 2004; Vielreicher et al., 2010), which are petrogenically associated with younger 2.64 Ga lamprophyre dykes (Woods, 1997). The monzodiorite to tonalite porphyry dykes have been related to numerous calc-alkaline stocks and dykes that intruded along the Golden Mile and Boulder-Lefroy Fault systems between Kalgoorlie and Kambalda (O'Beirne, 1968; Perring et al., 1991), some of which are associated with distinct skarn alteration (Mueller, 2007).

4. Structural history

The Kalgoorlie Gold Field is hosted in a thrusted and folded sequence of rocks that are dissected and offset by the regionally NNW-trending Boulder Lefroy-Golden Mile Fault zone that can be traced over a strike length of about 100 km (e.g. Swager, 1989; Swager et al., 1995; Weinberg et al., 2005). The structural history of the Gold Field has been studied by many (see reviews in Woodall, 1965; Travis et al., 1971; Mueller et al., 1988; Clout et al., 1990; Bateman et al., 2001; Mueller, 2015), and despite some disagreement on the timing of, or movement on, specific structures, there is general agreement on the sequence of deformation events, which has been used as a basis for regional correlations (Table 3). In a traditional scheme, following initial extension (De) and extrusion of ultramafic/mafic (Kambalda Sequence) to intermediate/felsic volcanic and volcaniclastic rocks (Kalgoorlie Sequence), thrust stacking and associated folding led to large-scale stratigraphic repetitions (D1). The rocks were then further folded, sheared and faulted during ENE–WSW to E–W compression associated with D2 to D4 (Table 3). The polyphase deformation defined as D2 to D4 is described as the product of the Kalgoorlie Orogeny (Weinberg and van der Borgh, 2008), or multiple discrete deformation events (Bateman et al., 2001) that record the accretion of the Kalgoorlie Terrane to the Proto-Yilgarn craton.

The widespread structural geometry of the Kalgoorlie Gold Field is the result of D2 deformation, when the regional stratigraphy and D1 thrusts were tilted into the current steep attitude, overprinted by a penetrative, subvertical foliation, sheared, faulted and folded. Shearing is variably described as sinistral (Mueller et al., 1988), sinistral-reverse (Bateman et al., 2001), or dextral reverse (Clout et al., 1990). The main D2 structures include upright folds and anastomosing shear zone systems and faults, which are cross-cut, reactivated and locally offset by D3 dextral reverse faults and shear zones. These and other D2 structures were subsequently reactivated during brittle deformation during D4, which was responsible for the development of steep, NNE-striking, dominantly right-lateral faults with a minor reverse movement, and formation of quartz-dominated veins and vein stockworks (Table 3). Mapped displacements across D4 faults are in the order of a few hundred metres at most (Bateman et al., 2001).

Table 1
Summary of sub-volcanic porphyry dykes that intrude the Kalgoorlie Gold Field (after Stillwell, 1929; Mueller et al., 1988; Clout et al., 1990; Woods, 1997; Vielreicher et al., 2010).

Rock type	Characteristics	Relationship with gold	Rock age (Ma)	Reference to age date
Lamprophyre dykes	Late deformation, mica lamprophyre, kersantite	Cut and are cut by Green Leader; Cut by Charlotte style	2642 ± 6[a] 2637 ± 20[b]	McNaughton et al. (2005) McNaughton et al. (2005)
Hornblende porphyry dykes	Local dyke swarm strikes N18°E/74°SE; Syn-deformation, variably metamorphosed, fractionated	Cut and are cut by Fimiston-style lodes; Cut by Charlotte-style lodes	2646 ± 13[a] *(2663 ± 11*[c] and *2674 ± 6*[a] *xenocrysts*[d]*)*	Vielreicher et al. (2010) *Gauthier et al. (2004)* *Kent and McDougall (1995)*
Feldspar porphyry dykes	suite of sub-alkaline to alkaline plagioclase-hornblende- and hornblende-phyric andesite dykes; monzodiorite-granodiorite-tonalite in composition; belong to high-LILE subgroup of the Mafic Group of intrusive rocks (cf Champion and Sheraton, 1997)	Cut by both Fimiston- and Charlotte-style lodes	2650 ± 6[a] *(2676 ± 3*[c] *xenocrysts*[d]*)*	Vielreicher et al. (2010) *Gauthier et al. (2004)*
Quartz-albite porphyry dykes and sills	Syn-volcanic, structurally early, pre-gold, calc-alkaline plagioclase-phyric rhyodacite sills and dykes; feeder dykes to volcanic units in the Kalgoorlie Sequence	Cut by both Fimiston- and Charlotte-style lodes	2673 ± 3[a] 2671 ± 10[a] 2669 ± 6[a] 2669 ± 17[a]	Yeats et al. (1999) Vielreicher et al. (2010) Vielreicher et al. (2010) Yeats et al. (1999)
Basalt	Syn-volcanic, tholeiitic dykes	Cut by both Fimiston- and Charlotte-style lodes		

[a] U-Pb SHRIMP ages on zircon; [b] U-Pb SHRIMP ages on monazite; [c] U-Pb TIMS age on zircon; [d] Ages from Kent and McDougall (1995) and Gauthier et al. (2004) have been reinterpreted to include a xenocrystic component by Vielreicher et al. (2010). These ages are shown in *italics* in the Table.

Table 2
Summary of deformation histories proposed for Kalgoorlie, highlighting the complexity and difficulty in defining a single structural development history. Please note that the DE to D4 annotation denotes the sequence of events as described by the corresponding authors.

	De	D1	D2	D3	D4
Swager (1997)	Low angle shearing on greenstone-granitoid contacts, N to S movement, local poly-directional extension and local recumbent folds; volcanism, plutonism, domes	D1 thrusting: sequence repetition, recumbent folds, S to N major thrust stacking followed by post-D1 and pre-D2 E—W extension: roll over anticlines, synclinal clastic basins	D2 regional ENE—WSW compression: upright folds, steep S2 foliation, domain-scale thrusting, inversion of extensional structures followed by E—W extension on Ida Fault, post metamorphic orogenic collapse	D3 E(NE)-W(SW) compression: strike and reverse slip faults, *en echelon* folds	D4 E-W compression: dextral-reverse oblique faults
Weinberg et al. (2003, 2005)	Post 2700 Ma D1e Extension: E—W directed, N to S extrusion of komatiites, bimodal volcanism, nappes, domes	Pre 2670 Ma D1 Compression: thrust stacking, stratigraphic repetition, deformation of eastern gneiss	2670—2650 Ma D2e Extension: subsidence of deep marine basin, granite magmatism, doming of eastern gneiss Post 2655 Ma D2 Compression: NNW—SSE upright folds, steep S2 penetrative foliation, granite magmatism, active buoyancy driven doming during folding, doming of eastern gneiss	D3 Transpression: mainly ductile sinistral reverse shears/faults, *en echelon* folds, intensification of S2 foliation	Pre 2640Ma D4 Compression: brittle NNE- SSW dextral reverse shears and faults, locally N-S and NNE-SSW
Mueller et al. (1988) Mueller and Muhling (2013), Mueller (2015)		D1 Regional folds upright and NW-striking, 20°SE-plunging (e.g. Kalgoorlie Syncline and Anticline); Folds are vertical—isoclinal at Mt Charlotte to upright and tight in the Golden Mile.	D2 Sinistral strike-slip transcurrent shear zones with D-, P-, P′-, R-shears; second generation folding where structures converge; Boulder-Lefroy and Parkeston Faults form as principal shear zones; oblique slip on Golden Mile Fault as subsidiary of Boulder-Lefroy Fault; folding of Golden Mile Fault as shearing progresses on principal shears; doming of Kalgoorlie Anticline axis; incl. Hannans North Shear; D2 pyrite-telluride bearing gold lodes.	D3 Dextral thrusts: displace the steeply- dipping D2 structures; includes N25—30°W/50—55°SW Neptune and Flanagan Thrusts	D4 Dextral strike-slip faults: north-striking; Golden Pike and Adelaide faults; Golden Mile Fault offset; R-shears; reactivation of D2 shears; tensional quartz veins and stockworks; reactivation of Boulder-Lefroy Fault
Clout (1989)		D1 multiphase, superimposed thrusting (Paringa Basalt-Golden Mile Dolerite contact, and Flanagan Fault set), macro- and megascopic folding (early Kalgoorlie Syncline and Anticline and late Boomerang Anticline) and steep reverse faulting (early Golden Mile Fault and later Boulder Faults)	D2 N-trending, oblique, anastomosing faults with dextral net slip (Adelaide and Golden Pike Faults); mesoscopic shear system between Adelaide and Golden Pike Faults; isolated shear zones accommodate movement on faults	D3 upright anastomosing cleavage; local small scale folds; stylolites, syntectonic fibre growths; micro- and macro-extension veins; pressure solution cleavage; late brittle vein stockworks; late to post-D3 brittle cross faults (e.g. Hannans Star Fault)	
Bateman et al. (2001)	De transfer and extensional faults; major regional faults; basin margin faults syn-deposition of Black Flag Beds (e.g. Adelaide and Titicaca Faults	D1 NE-over-SW thrusting; Golden Mile Fault and Golden Mile Anticline as nappe/hanging-wall anticline with strain partitioned between fault and fold.	D2 regional NE—SW compression; upright folds; conjugate E—W oblique (sinistral-reverse) faults; tilting of stratigraphy; steep NNW-reverse faults subparallel to stratigraphy and folds; incl Mt Hunt, Boulder, Abattoir East, Flanagan, Neptune and Shea Faults; pervasive N—S, subvertical axial planar cleavage; 3 foliations from progressive development of Celebration Anticline; incl. movement on Golden Mile Dolerite-Paringa Basalt contact, Oroya Hangingwall and Footwall Shears	D3 dextral, strike-slip, NNE, steeply NW-dipping, sigmoidal faults sub-parallel with stratigraphy; Golden Pike, Adelaide and Loongana Faults; reactivation of Boulder Fault - Boomerang Anticline; Boorara Shear as bounding fault to local-scale antithetic dextral reverse faults- e.g. Kalgurli Fault	D4 NNE, vertical to steep NW-dipping, dextral oblique slip faults; Charlotte and Hannans Star Faults; SW-plunging mineral lineation; sheeted vein arrays; reactivation of D2 faults, e.g. Flanagan, Neptune and Shea Faults

Table 3
Summary of the main characteristics of Fimiston- and Mt Charlotte-style gold mineralization.

	Fimiston (including Green Leader)	Mt Charlotte
Structural style	Ductile-brittle, stringers, veinlets, breccias, cataclasites	Brittle vein stockwork
Structural timing	Syn D2 shearing	Variably described as D3/4 faulting
P-T estimates from mineralogy	305 to 390 °C & 110 to 290 MPa[a] Peak > 300 °C [b]	325–375 °C & 100 MPa [c] 365 °C and 200–400 MPa[d]
Metamorphic timing	Post-peak	Post-peak
Alteration	Dominant – sericite, carbonate, albite Lesser – roscoelite, rutile, tourmaline, hematite, magnetite	Type 1: Sericite-ankerite-albite-rutile Type 2: Albite-ankerite-sericite-rutile Type 3: Albite-ankerite-rutile-sericite Lesser – scheelite
Ore mineralogy	Dominant – pyrite Lesser – telluride minerals, tetrahedrite-tennantite, arsenopyrite, galena, sphalerite	Dominant – pyrite/pyrrhotite Lesser – telluride minerals, galena, sphalerite
Zonation	Increase in Au/Ag in native gold, and Sb/Au in tennantite-tetrahedrite with depth[e]; Increase in montbrayite ($(AuSb)_2Te$) outwards, and telluroantimony (Sb_2Te_3) at depth.[b] Increase in Sb distal to lodes	Concentric alteration: increase in albite and pyrrhotite, and decrease in sericite and pyrite towards centre and at depth[c]
Element addition	K, Rb, Sb, S, Te, V, Ba[f]	K, Rb, Cs, Li, Ba, W, Ca, Sr, Mg, V, Te
Age (NB Ar/Ar ages are quoted with total uncertainties, i.e. analytical and systematic)	2643 ± 13 Ma (Ar/Ar sericite in ore zone)[g] 2642 ± 6 Ma (Pb/Pb zircon in syn-ore lamprophyre)[h] 2641 ± 13 Ma (Ar/Ar sericite in ore zone) [g] 2638 ± 18 Ma (Pb/Pb monazite in ore zone) [i] 2637 ± 20 Ma (Pb/Pb monazite in syn ore lamprophyre) [h] 2632 ± 12 Ma (Pb/Pb monazite in ore zone) [i] 2625 ± 28 Ma (Ar/Ar sericite in ore zone) [i] 2610 ± 4 Ma (Ar/Ar sericite in ore zone) [j]	2655 ± 13 Ma (Pb/Pb xenotime in ore zone) [w] 2644 ± 11 Ma (Pb/Pb xenotime in ore zone) [i] 2617 ± 11 Ma (Ar/Ar sericite in ore zone) [g] 2614 ± 13 Ma (Ar/Ar sericite in ore zone) [g]
Fluid inclusions	Lake View: 3 phase H_2O-CO_2, low salinity (0.0–1.8 wt.% NaCl equiv.), T_h = 196–330 °C, P = 150–400 MPa[k] Paringa: 3 phase H_2O-CO_2, low salinity (3.1–5.5 wt.% NaCl equiv.), T_h = 280–256 °C, P = 150–180 MPa [k] Fimiston: H_2O-CO_2-CH_4, low to moderate salinity (0–13 wt.% NaCl equiv.), T = 110–250 °C, P = 10–26 MPa and H_2O with 6–23% NaCl equiv.) [l] Oroya: H_2O-CO_2-CH_4, low salinity (<5 wt.% NaCl equiv.), T_h = 225–355 °C, P = 120–280 MPa[l]	Stages 1, 2 and 3: 3 phase H_2O–CO_2, 2.0–4.2 wt.% NaCl eq., T_h = 210–360 °C, P = 160–220 MPa[k] Stage 3: 2 phase H_2O-CO_2-CH_4 & 2 phase H_2O, low salinity (4.1–5.5 wt.% NaCl eq.), T_h = 265–290 °C[k] Type 1 vein: 3 phase H_2O–CO_2, low salinity (<4 wt.% NaCl equiv.), T_h = 210–316 °C and liquid-rich H_2O with T_h = 98–313 °C[m] Type 2 vein: 2 phase H_2O-CO_2-CH_4, T_h = 218–323 °C and liquid-vapour H_2O with T_h = 220–283 °C[m] Type 3 vein: liquid + vapour H_2O-CO_2-CH_4, T_h = 235–439 °C & liquid-rich H_2O with T_h = 220–440 °C[m] Late secondary liquid-rich H_2O-CH_4 with T_h = 239–286 °C[m]
$\delta^{34}S$ values	−10 to −4‰[f]; −10 to +10‰[n]	1.0 to 4.2‰[o]; 2.2 to 4.3‰[p]
$\delta^{18}O$ values	8.6–12.3‰ (alteration)[p]; 13.3–13.5‰ (vein quartz) [p]; 6.5 ± 2.0‰[p]; 11.0–13.9‰ (wallrock)[l]; 12.6–13.7‰ (whole rock)[l]; 13.0–15.0‰ (vein)[l]; 14.5–15.0‰ (quartz)[l]	11.3 ± 0.3‰ (Charlotte) [p] 11.4 ± 0.5‰ (Reward) [p]
$^{87}Sr/^{86}Sr$ composition	0.704 to 0.705[r]; 0.7013 to 0.7016 (primary sulphate)[l]; 0.7048 to 0.7049 (late sulphate)[l]; 0.7018 to 0.7052 (secondary sulphate)[l]; 0.7014 (tourmaline)[q]	0.70134 to 0.70145[s] 0.7014 to 0.7028[q] 0.7014 to 0.7016 (vein scheelite)
$\delta^{13}C$ composition	No4 lode: −4.1 to 1.5[t]	Reward: −7.6 to 12.7[t] Charlotte: −7.9 to 8.8[t]
$^{206}Pb/^{204}Pb$	13.636 to 14.752[u]	13.682 to 13.840; 14.773 to 14.824 [v]
Telluride geochemistry	Early calaverite-gold (300 °C); log fTe_2 = −11.4 to −6.8; log fS_2 = −12.6 to −5.5; Later petzite-hessite (<170 °C) [b]	Early gold-hessite assemblage (250–300 °C), log fTe_2 of −11.5 to −10[b]
ε_{Nd} values		3.3 to 9.0 at 2602 Ma[s]

[a] Based on sericite geobarometry and arsenopyrite and chlorite geobarometry (R. Vielreicher; unpublished data); [b] Shackleton et al. (2003); [c] Mikucki and Heinrich (1993); [d] Mueller (2015); [e] Golding (1978); [f] Phillips (1986); [g] Kent and McDougall (1995); [h] McNaughton et al. (2005); [i] Vielreicher et al. (2010); [j] Heath (2003) mean age of 14 analyses of 14 samples of sericite and roscoelite with individual plateau-like ages of 2562 ± 12 to 2622 ± 12 Ma; [k] Ho (1987), Ho et al. (1990); [l] Clout (1989) NB. secondary sulphate in Mt Charlotte-style extensional veins. Also P-T calculations described as out of date by Bateman et al. (2001); [m] Mernagh (1996); [n] Hagemann et al. (1999) noted variations between lodes; [o] Clout et al. (1990); [p] Golding et al. (1990a,b,c) for alteration and vein quartz; [q] Mueller et al. (1991); [r] Turek and Compston (1971) for gold and regional granites; [s] Kent et al. (1995); [t] Golding et al. (1987); [u] McNaughton et al. (1992); [v] Dahl et al. (1987); [w] Rasmussen et al. (2009).

5. Nature of ore bodies

Gold mineralization is hosted in all rock types within the Gold Field, but the Golden Mile Dolerite is the principal host to ore. The distribution and style of gold mineralization and lode geometry in all deposits is controlled by a complex interplay of structural development, rheological and chemical contrasts in host rocks, and dyke intrusion (e.g. Nixon et al., 2014).

In the Golden Mile, gold is mined from an array of ductile to brittle-style, stringer-, vein- and breccia-lodes that have been classified into four groups based on orientation; namely Main (320/90-85SW), Caunter (280–300/70SSW), Easterly (160/70-90ENE), and Cross (220–230/65-80SE) lodes. In contrast, gold at Mount Charlotte is mined from stockworks of coarse-grained sheeted veins that are spatially associated with brittle dextral-reverse faults. The other deposits of the Gold Field contain at least one of these two "end-member" ore types, which have been described as Fimiston- and Mt Charlotte-style (Table 3).

5.1. Fimiston-style ore

Fimiston-style ore comprises approximately-planar, steeply-dipping lodes of fine-grained silica-sericite-sulphide-telluride bearing quartz-carbonate veinlets, crackle- and cockade- breccias, banded chalcedonic quartz-carbonate veins, and stringer zones that define millimetre- to centimetre- scale proto- to ultramylonites that are interlayered with, or grade into, lenses of microbreccia and cataclasite (Fig. 4; Clout, 1989; Bateman et al., 2001; Gauthier et al., 2004). Lodes are characterized by variably-foliated ankerite/dolomite/siderite − quartz − sericite − pyrite − Fe/Ti-oxides (locally as boxworks after Ti-magnetite), ± Fe-chlorite, ± tourmaline alteration. Alteration is described as zoned with an outer kilometre-wide envelope of chlorite-calcite ± ankerite, inner ankerite and siderite zone that extends for over 100 m, and proximal gold-bearing, pyrite-sericite zone with ankerite ± siderite. However, Nixon et al. (2014) recently emphasized the strong lithological control on alteration based on detailed mapping and core-logging (Fig. 3). Hence, alteration mineralogy as well as its intensity is strongly controlled by the interplay of structure and lithology (Phillips, 1986; White et al., 2003). Despite the wide zone of carbonate ± chlorite alteration, the abundant anastomozing inner pyrite-rich zones suggest that fluid flow was along multiple conduits that were accompanied by multiple discrete alteration haloes. As fluid flow continued, the alteration haloes extended and coalesced. The final alteration halo is, therefore, a composite of alteration from a mineralizing fluid that entered the rock via a complex network of multiple conduits (White et al., 2003).

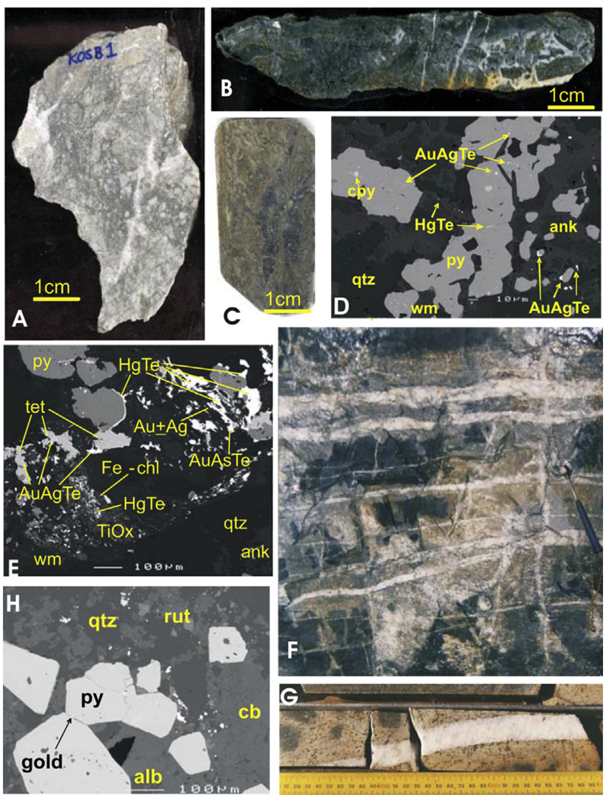

Figure 4. Examples of contrasting ore styles within sericite-altered Golden Mile Dolerite. (A) Brittle-ductile Fimiston-style ore from the Oroya Lode at the contact with Paringa Basalt in the eastern lode system at the Golden Mile, showing clasts of sericite altered host rock within a cataclastic matrix of fine-grained sulphide-dominated rock (dark grey/black; grab sample from Fimiston Pit, <10 g/t Au). (B) Brittle Fimiston-style ore from drill core through the Ivanhoe # 2 Lode in the western lode system at the Golden Mile, showing gold, telluride and sulphide-bearing quartz-carbonate breccia (Drillhole JUGD10, 360 m, 72 g/t Au). (C) Thin-section off-cut of more-ductile Fimiston-style gold-rich sample (from 35 cm interval returned grade of 183–203 g/t Au) from the Paringa Lode in the Eastern Lode System showing disseminated sulphide (yellow brassy) and telluride (grey silver) minerals (Drill hole PRD72, 200.1 m). (D) Backscattered electron image showing inclusions of Au-Ag- and Hg- telluride together with chalcopyrite within fine-grained pyrite (py) intergrown with sericite (wm), zoned ankerite (ank; increased iron in rims) and quartz (qtz) in high gold grade Fimiston-style ore sample (Drillhole JUGD10, 360 m, 72 g/t Au). (E) Backscattered electron image showing typical association of gold (Au ± Ag) with telluride minerals (unidentifed gold-arsenic telluride -AuAsTe, krennerite - AuAgTe & coloradoite - HgTe) as inclusions and along cracks in, and rims on, pyrite (py) and tetrahedrite (tet), intergrown with chlorite (Fe-chl), Fe-zoned ankerite (ank; increased Fe in rim), rutile (TiO_x) and sericite (wm) in altered dolerite (Drill hole PRD70, 227.3 m, 180–184 g/t Au). (F) Underground exposure of typical, brittle, sheeted Mt Charlotte-style veins and associated bleached alteration haloes from Level 21 in the Charlotte Deeps orebody at the Mount Charlotte mine. (G) Core sample of narrow Mt Charlotte-style quartz-carbonate vein within sericite-pyrite altered dolerite (Drill hole MC2235, 93.6 m). (H) Backscattered electron image showing the simple mineralogical association of gold with euhedral pyrite (py) and alteration minerals albite (alb), carbonate (cb), quartz (qtz), rutile (rut) in Mt Charlotte style ore (grab sample from the Charlotte Deeps orebody underground on Level 21 at the Mount Charlotte deposit).

Gold is typically refractory, either as micron-scale inclusions in fine-grained (less than 0.1 mm) inclusion-rich pyrite or as inclusion-poor auriferous pyrite. Hence, the occurrence of fine-grained pyrite is directly related to gold distribution. In high-grade zones (up to 10,000 g/t, typically >50 g/t), native gold, tellurium with a range of telluride minerals (Shackleton et al., 2003) as well as chalcopyrite, arsenopyrite (particularly in the Aberdare Lodes), tennantite-tetrahedrite, sphalerite and galena, are closely associated (e.g. Fig. 4). These zones are characterized by addition of CO_2, K, Rb, S as well as Au (-B), Te, V and Ba (Phillips, 1986).

Local bonanza grade shoots (up to 100 000 g/t Au) are spatially related to carbonaceous metasedimentary units, and are characterized by abundant free gold associated with native tellurium and rarely, mercury (Weller et al., 1998), together with disseminated pyrite and numerous Au-Ag, Ni, Hg, Pb, Sb-bearing telluride minerals (Stillwell, 1929; Scantlebury, 1983; Clout et al., 1990). These zones termed "Green Leader" (Larcombe, 1912) are also located at the core of some of the more typical Fimiston-style lodes and are marked by a complex alteration assemblage that includes the distinctive green roscoelite with ankerite, calcite, siderite, sericite, V-Ti-bearing Fe-oxides, pyrite, chalcopyrite, arsenopyrite, tennantite-tetrahedrite, sphalerite and galena (Stillwell, 1929; Scantlebury, 1983). In most cases, Fimiston-style gold lodes grade into the Green Leader zones, also termed Oroya-style after the well documented, pipe-shaped, gently-plunging Oroya Shoot within the Paringa Basalt that follows a graphitic sedimentary unit at the contact with the Golden Mile Dolerite (Bateman et al., 2001). Steadman et al. (2015) recently described gold in syn-sedimentary to diagenetic zoned pyrite nodules within these graphitic units and raised the question whether a sedimentary source for gold may have added to the gold budget, but the units are volumetrically too thin to provide a significant source of gold for the giant Gold Field.

Zoning within the Golden Mile is evident, with an overall increase in Sb/Au in the tennantite-tetrahedrite group minerals, as well as an increase in Au/Ag ratio in the free gold with depth (Golding, 1978). Associated with this is a zonation in the telluride mineralogy, with increasing montbrayite ($(AuSb)_2Te$) laterally, and telluroantimony (Sb_2Te_3) at depth (Shackleton et al., 2003).

5.2. Charlotte-style ore

Charlotte-style ore describes stockworks of locally coarse-grained, open-space textured, dilational, quartz-, carbonate-, albite- and scheelite- bearing sheeted veins with distinct alteration haloes (Fig. 4; Clark, 1980; Ridley and Mengler, 2000). Individual veins vary in thickness from a few millimetres to several metres thick, contain multiple generations of quartz growth (Clark, 1980), are mutually crosscutting, and are preferentially developed within rheologically strong units, particularly the coarse-grained granophyric Unit 8a of the Golden Mile Dolerite, but also Units 7 and 9, and porphyry dykes hosted within the Hannans Lake Serpentinite. The veins are described as a network of extension and shear fractures that are associated with late steep- and gently-dipping, northerly-trending fault sets that offset the regional NW-trending foliation (e.g. Clark, 1980; Ridley and Mengler, 2000; Weinberg et al., 2005; Mueller, 2015). At Mount Charlotte, the ore mineralogy is relatively simple (Fig. 4), with gold associated with pyrite, pyrrhotite, telluride minerals, ankerite, sericite and quartz, and ores are free-milling. Gold is predominantly sited at vein contacts or in the pyritic haloes where it occurs as 5–15 μm grains in fractures in pyrite or at contacts between pyrite and gangue minerals. Distinct alteration zones surround the veins with associated enrichments in K, Rb, Cs, Li, Ba, Ca, Sr, Mg, Ni, V, Cr, W, Te, and Au (Mueller, 2015). Variations in modal alteration mineralogy (Clark, 1980) changed systematically in the deposit (Mikucki and Heinrich, 1993);

Type 1: Pyrite-muscovite alteration comprises an inner bleached alteration halo (up to ~50 cm from vein margins) of quartz–ankerite–white mica–albite–rutile–pyrite that grades out through an outer diffuse contact zone (50–100 cm from vein margins) that contains additional chlorite and ilmenite, to least-altered protolith. Although this alteration style contains high gold-grades locally, it is mostly at the periphery and outside of the bulk-mineable orebody.

Type 2: Pyrite-pyrrhotite alteration is similar to the pyrite-muscovite alteration with the added occurrence of pyrrhotite in the outer diffuse contact zone (i.e. up to 100 cm from vein margins), and an increase of albite at the expense of muscovite in the inner bleached zones. It is the dominant alteration type in the economic ore-zone at the highest levels of the deposit, is common along the periphery of the orebodies at intermediate levels, and is associated with isolated, distal veins in the deeper part of the deposit (Charlotte Deeps).

Type 3: Pyrrhotite-albite alteration includes zones where pyrrhotite occurs in the inner and outer parts of the alteration envelopes, and there is a marked increase in albite in the inner zone. It dominates within the core of the stockwork and at the deeper levels of the mine.

Mikucki and Heinrich (1993) described the distribution of these alteration haloes as unrelated to lithological variations or structures (except, in part the Flanagan Fault), but rather is centred on areas of highest density veins. However, Nixon et al. (2014) described the variation in carbonate and sulphide mineralogy as a function of the host rock, with pyrrhotite restricted to ultramafic host rocks, and base-metal sulphides present in more intermediate to felsic and sedimentary host rocks.

6. Mineralogy

6.1. Mineral paragenesis

The rock sequence at Kalgoorlie is metamorphosed to upper greenschist facies mineral assemblages (350–400 °C; Mikucki and Roberts, 2003). Primary igneous and sedimentary textures are locally well preserved in low strain zones (e.g. Bartram, 1969; Clout et al., 1990; Mikucki and Roberts, 2003), but original igneous phases such as pyroxene, plagioclase and titanomagnetite in the Golden Mile Dolerite (main host to gold mineralization) are replaced by actinolite (±biotite)-albite/epidote-ilmenite/titanite-quartz (Clout et al., 1990). The metamorphic assemblage is increasingly overprinted and replaced by the gold-related alteration with proximity to lodes (Scantlebury, 1983; Phillips, 1986; Clout, 1989; Clout et al., 1990; Shackleton et al., 2003; Mernagh et al., 2004). A generalized mineral paragenesis (Fig. 5) within the altered and mineralized Golden Mile Dolerite at the Golden Mile and Mt Charlotte deposits indicate that the bulk of the gold was deposited relatively late in the paragenesis in both ore systems. However, the relative timing of specific mineral deposition is complex and varies in detail, particularly across lodes and lithological contacts (R.M. Vielreicher and S.G. Hagemann, unpublished data).

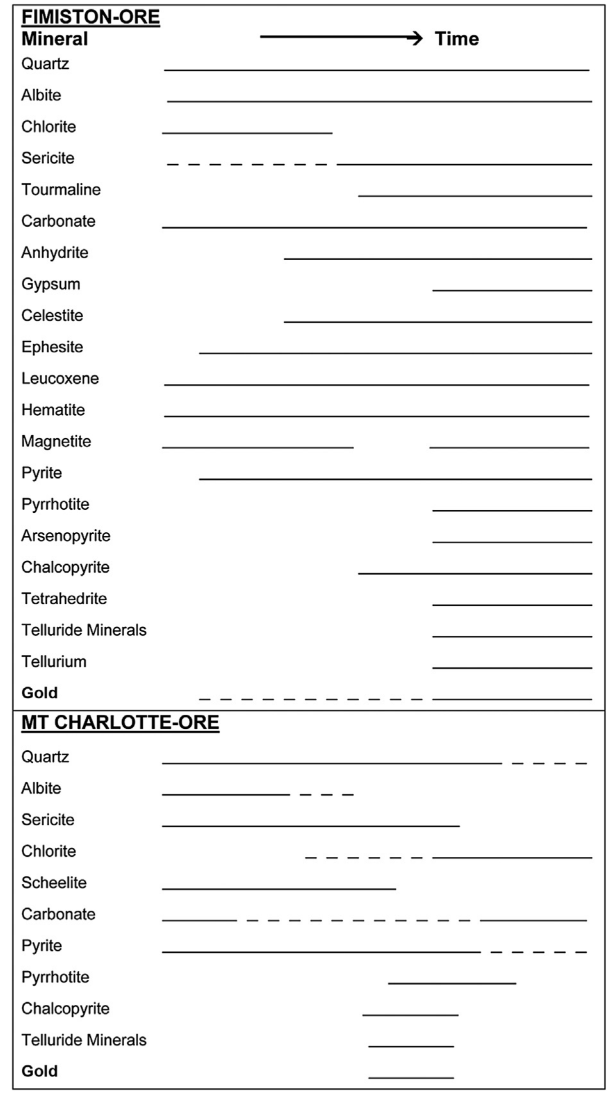

Figure 5. Paragenetic mineral sequence of the Fimiston lodes in the Golden Mile and Mt Charlotte lodes (after Clout et al., 1990; Shackleton et al., 2003; Mernagh et al., 2004; RM Vielreicher and SG Hagemann, Unpubl. Data).

6.2. Mineralogical constraints on P-T conditions of gold mineralization

Petrographic studies indicate that the gold-related alteration assemblages in both the Golden Mile and Mt Charlotte just postdate peak regional greenschist-facies metamorphism (Mikucki and Roberts, 2003). The mineralogy of alteration associated with the Fimiston lodes supports influx of an aqueous–CO_2 dominated fluid that reacted with the metabasic hostrocks and caused breakdown of actinolite to chlorite and carbonate. Sericite in the proximal alteration zones is the result of potassium addition from the fluid (White et al., 2003), and pyrite is the result of sulphidation of Fe in the host rocks (Neall, 1987). Mineral equilibria studies show that the alteration assemblages are consistent with equilibrium with a single fluid of composition $X_{CO_2} = CO_2/(CO_2 + H_2O) = 0.1$ to 0.25 (outer zones) and 0.25 (inner zones) at temperatures of 315 to 320 °C (White et al., 2003). These temperatures fall within the range defined by arsenopyrite and chlorite geothermometry from alteration assemblages from Lake View, Oroya and Great Boulder Main Lodes in the Golden Mile from 305 to 390 °C (Table 3). Sericite geobarometry on the same samples indicates pressures of 110 to

290 MPa (R.M. Vielreicher and S.G. Hagemann, unpublished data). In line with these calculations, Shackleton et al. (2003) suggested that the gold + calaverite + petzite and minor late hessite in the Golden Mile were deposited by a fluid cooling from 300 °C to below 170 °C.

At Mt Charlotte, temperature and pressure estimates calculated from mineral stability fields and compositions indicate temperatures and pressures of 325 to over 400 °C and 100–400 MPa with a deposit-wide thermal zonation of up to +100 °C from top to bottom (Mikucki and Heinrich, 1993; Mueller, 2015). Mueller and Muhling (2013) constrained an upper temperature limit for rare, telluride-bearing mineralization that structurally predates the main gold-bearing veins, by the incongruent melting point of krennerite (382 ± 5 °C) and sylvanite (354 ± 5 °C; Cabri, 1965). Alteration mineralogy is consistent with the same depositional mechanisms as at the Golden Mile, with gold deposited during wall rock sulphidation in overlapping vein selvages zoned from deep albite–pyrrhotite (3 g/t Au) to upper sericite–pyrite assemblages (5 g/t Au bulk grade; Mikucki and Heinrich, 1993; Mueller, 2015).

7. Fluid characteristics

Several fluid inclusion studies have been carried out on the Golden Mile and Mt Charlotte deposits. However, the quality of the data is variable, and in the Golden Mile, in particular, the data are not all geologically well constrained as samples are from different lodes within this extensive orebody, hence making it difficult to reconcile all the results.

7.1. Golden Mile

Clout (1989) described fluid inclusions from Fimiston-style mineralization as a mixture of both low to moderate salinity, aqueous–carbonic fluid inclusions with 5 to almost 100 mol.% CO_2 that underwent phase separation at around 110 to 250 °C and 10 to 26 MPa, and co-existing variably saline aqueous inclusions (up to 23 wt.% NaCl equiv.; Table 3). A second study of fluid inclusions in quartz from high gold-grade, telluride-bearing and telluride-absent samples from Paringa and Lake View lodes showed marked variation between lodes (summarized in Ho, 1987). Quartz from Lake View contains very low salinity, CO_2-H_2O inclusions, with variable CO_2/H_2O of 1 to 4, that homogenize between 280 and 356 °C with trapping pressures (based on the system H_2O–CO_2) of 196 to 330 MPa. In contrast, quartz from the Paringa Lode contains a continuum of low-salinity inclusion types that vary between two-phase aqueous and CO_2-CH_4 inclusions that have a thin outer film of H_2O, and display a narrower range in both trapping pressure (150 to 180 MPa) and homogenization temperatures (T_h: 280 to 356 °C). The difference in the datasets is significant in that Clout (1989) calculates higher salinities for some aqueous inclusions and extremely low pressures (down to 10 MPa) during phase immiscibility (Table 3), which he uses to support an epithermal model for Golden Mile gold mineralization. However, Bateman et al. (2001) questioned the validity of the *P-T* values as the calculation methodology of Clout (1989) has since been discounted. In addition, such extremely low pressure conditions have not been recorded by any other author using any other method on ore samples from the Golden Mile.

7.2. Mt Charlotte

Different generations of quartz from Mt Charlotte stockwork veins (as defined by Clark, 1980) contained two-phase, low salinity, aqueous to aqueous-carbonic fluid inclusions with T_h of 210 to 360 °C and trapping pressures of 150 to 220 MPa (summarized in Ho et al., 1990). A more recent study by Mernagh et al. (2004) related the fluid inclusion data to the style of alteration surrounding the veins (Mikucki and Heinrich, 1993), and identified a distinct, deposit-scale thermal trend (Table 3). The fluid inclusions in veins in the upper and distal parts of the deposit (Type 1 alteration) include three-phase H_2O–CO_2 inclusions that homogenize at 210 to 316 °C, whereas veins in the central and lower levels of the deposit contain two-phase aqueous-carbonic (H_2O–CO_2–CH_4) inclusions with T_h of up to 440 °C (Type 3 alteration) indicating a temperature difference of up to 200 °C across the deposit. The chemical composition (H_2O:CO_2:CH_4:NaCl) of the inclusions, although highly variable (particularly CH_4:CO_2), does not vary in a systematic manner. Mernagh et al. (2004) surmised that these observations are the result of gold deposition by desulphidation of bisulphide complexes due to reaction with Fe-rich wallrocks to form pyrrhotite and pyrite, as previously suggested (e.g. Neall, 1987). These reactions are strongly temperature-dependent, and also account for the variation in pyrrhotite and pyrite in the deposit. Furthermore, the relatively high grade of gold in the Mt Charlotte orebody is explained as a result of the unusually steep temperature-gradient along the fluid-flow path through the vein network (Mernagh et al., 2004).

8. Isotope compositions

8.1. Stable isotope compositions

Conventional sulphur isotope analyses on pyrite from Golden Mile mineralization have been performed by Lambert et al. (1984), Golding et al. (1987, 1990c), Phillips et al. (1988) and Clout (1989) and revealed distinctively negative $\delta^{34}S$ values (down to −10‰; Table 3), that contrast with most published values for other Neoarchean lode-gold deposits (Colvine et al., 1988). Lambert et al. (1984) and Phillips et al. (1988) explained the range in $\delta^{34}S$ values in terms of oxidation of reduced sulphur to sulphate during reaction of an ascending, reduced CO_2-rich fluid with the magnetite-rich Unit 8 of the Golden Mile Dolerite. Phillips et al. (1988) argued that the resulting small changes in the $f(O_2)$of the fluid and wallrock would result in considerable shifts in pyrite compositions to more negative $\delta^{34}S$ values. Clout (1989), on the other hand, invoked an oxidized ore fluid to explain the negative $\delta^{34}S$ values, one that was likely derived from either felsic magma or by oxidative metamorphism and dehydration of shear zones in the lower crust during CO_2 streaming (cf, Cameron, 1988). Using laser-based isotope analyses, which allows better resolution, Hagemann et al. (1999) confirmed the light values, but also noted a distinct heterogeneity in values across alteration zones and between the Oroya, Lake View and Great Boulder Main lodes. Pyrite distal to gold mineralization in all three lodes has similar $\delta^{34}S$ values within the range of −2 to +6‰. However, with proximity to gold mineralization, the $\delta^{34}S$ values differ from lode to lode. Pyrite from mineralized samples from the Oroya lode display a more restricted range in $\delta^{34}S$ values of 2 to 5‰, whereas, $\delta^{34}S$ values of pyrites from Great Boulder Main scatter (−4 to +9‰), and those from Lake View lode shift towards more negative values (−10 to +1‰) in line with previously published $\delta^{34}S$ values. Hagemann et al. (1999) also noted marked intragrain variations, and postulate that the variations in composition are evidence for multiple processes such as boiling and mixing, and multiple sulphur sources that acted during a protracted hydrothermal history in the Golden Mile.

In contrast with the Golden Mile, conventional sulphur isotope analyses of pyrite from Mt Charlotte ore yield a relatively restricted range of dominantly positive $\delta^{34}S$ values (1.0 to 4.3‰; Table 3), that are similar to many other Neoarchean gold deposits (e.g. Colvine et al., 1988).

$\delta^{18}O$ and δD values have been published for a range of regional, variably altered and mineralized samples from the Golden Mile (Table 3; Clout, 1989; Golding et al., 1990a,b). Clout (1989) calculated oxygen isotope values of 8.6 to 12.3‰ for quartz from alteration zones and 13.3 to 13.5‰ from veins. He used these values, in combination with hydrogen isotopic compositions of −35.5 to +5‰ and his fluid inclusion data, as evidence for the derivation of ore fluids from either seawater or low-latitude meteoric water, which isotopically exchanged with the wallrocks and/or a magmatic porphyry fluid. Golding et al. (1990a,b) analyzed a wide range of whole-rock through to vein quartz samples and obtained a more restricted range in $\delta^{18}O$ values (11.0 to 15.0‰; Table 3), and argued that the values are more consistent with a metamorphic origin for the ore fluids.

Oxygen isotope ($\delta^{18}O$) compositions of whole-rocks and quartz veins adjacent to the Charlotte Fault in the Charlotte and Reward orebodies at Mt Charlotte are virtually identical (Table 3; Golding et al., 1990a,b), with no evidence of temperature variation over the vertical interval (>300 m) of the vein stockwork system, suggesting that the veins formed from an isotopically homogeneous ore fluid over a small temperature range. However, Mernagh et al. (2004) re-assessed these $\delta^{18}O$ isotope data, and showed that there are variations in $\delta^{18}O$ that closely follow a fault-related indentation on the southern side of the Charlotte Fault, implicating the NW-trending strike-parallel and NE-trending oblique faults as ore fluid channelways. Furthermore, they also highlighted a zone of higher $\delta^{18}O$ whole-rock values coincident with the zone of Type 3 alteration: quartz veins near the centre of the orebody have $\delta^{18}O$ values around 11‰, whereas peripheral veins exhibit values ranging up to 13‰. The variation in $\delta^{18}O_{quartz}$ is interpreted to be the result of a gradient in fluid temperature (Mikucki and Heinrich, 1993) in the order of 55 °C (cf fluid-inclusion study of Mernagh et al., 2004).

8.2. Radiogenic isotope compositions

The Pb-isotopic character of the ores from the Golden Mile (Table 3) indicates that there has been equilibration with mafic-ultramafic rocks of the greenstones, with some contribution from an older more-radiogenic source (probably felsic crust; Golding, 1978; McNaughton et al., 1992). Furthermore, as there has been no net addition of Pb to the ore zones at the Golden Mile (Phillips and Gibb, 1993), it is interpreted that the Pb isotope data reflect the compositions of the host rock sequence and conduits more than the mineralizing fluid/s or metal sources.

Lead isotope compositions of samples from Mt Charlotte show a restricted range of mixing between host-rock and ore-fluid Pb (Table 3), and its evolutionary pathway is distinctly different to Pb in samples from the Golden Mile, suggesting diverse source regions and/or conduits for the Pb in the gold mineralizing fluids (Dahl et al., 1987).

Clout (1989) described three generations of sulphate minerals (primary, late and secondary) from the Golden Mile and presents Sr isotope data for each group (Table 3). The primary sulphates from Fimiston-style mineralization have low $^{87}Sr/^{86}Sr$ and low Rb contents, and are interpreted to be close to initial mantle values resulting from equilibration with mantle-derived rocks. The late (also Fimiston-style) and secondary (? related to Mt Charlotte-style veins) sulphate samples have progressively higher ratios and are taken to indicate either substantial differences in crystallization ages, or a greater contribution from Rb-rich radiogenic (crustal) sources of Sr. It is interesting that regionally, more radiogenic Sr and Pb isotopic compositions are most common in deposits closer to the granite-gneiss domains (McNaughton et al., 1992). Bateman et al. (2001) suggested that the more radiogenic nature of the late and secondary sulphate is the result of fluid mixing.

Strontium compositions in samples of Mt Charlotte ore cluster tightly between 0.7013 and 0.7016 (Table 3; Mueller et al., 1991; Kent et al., 1995). Kent et al. (1995) invoked a simple model of metamorphic devolatilization, which is rejected by Mueller et al. (1991) in favour of a magmatic-hydrothermal model where radiogenic Sr re-equilibrated with less-radiogenic Sr in mafic magmatic rocks such as the high-Mg monzodiorite intrusions ($^{87}Sr/^{86}Sr = 0.7016 - 0.7018$).

Carbonates from the No. 4 lode in the Golden Mile (mean = −3.3 ± 0.6‰; Table 3) and samples of district-scale alteration (means of −3.1 ± 1.1‰, −3.1 ± 0.9‰, −3.5 ± 2.1‰) at Kalgoorlie yield anomalously positive $\delta^{13}C$ isotope values, particularly when compared with other deposits in the Kalgoorlie Terrane (typically $\delta^{13}C$ of −5 to −7‰; Golding et al., 1987). Golding et al. (1987) dismissed a mechanism such as a redox shift in the $\delta^{13}CH_2CO_3(aq)$ of fluids containing magmatic CO_2 as suggested for other Neoarchean deposits (e.g. Timmins, Ontario, Colvine et al., 1988) because isotopic and mineralogical constraints on the fluid oxidation state indicate that it lies above the CO_2/CH_4 boundary. Instead, possible explanations put forward include mixing of CO_2 from dissolution of carbonate derived from at least two different carbon reservoirs such as mantle and metamorphic alteration, or high temperature re-equilibration with carbonated komatiites, with subsequent lower-temperature wall-rock alteration and carbonate deposition (Golding et al., 1987).

The distinct $\delta^{13}C$ compositional range in carbonate minerals (means of −4.8 ± 4.4‰ for Reward and −5.0 ± 3.2‰ for Charlotte samples; Table 3) from gold-related alteration at Mt Charlotte is similar to that at the Hunt and Victory mines in Kambalda, thereby highlighting the connection of these deposits with the through-going structural corridor of the Boulder-Lefroy Fault. Golding et al. (1987) concluded that these values are compatible with local CO_2 derived from reworking of mantle carbonate during regional, dynamothermal metamorphism. The carbonated komatiites along the Boulder Lefroy Fault zone are interpreted to be the result of direct mantle carbonation, but their composition is more isotopically homogeneous, and differs statistically from the Golden Mile data (Table 3), suggesting a regionally distinct source (Golding et al., 1987). This contrast is underlined by similar contrasts in the sulphur isotope compositions (e.g. Lambert et al., 1984), lead isotope ratios (e.g. Dahl et al., 1987) and pyrite trace-element compositions (Phillips, 1986).

9. Timing of gold mineralization in the Kalgoorlie Gold Field

There is a longstanding controversy regarding the timing of gold mineralization in the Kalgoorlie Gold Field. Some authors describe Fimiston-, Oroya- and Mount Charlotte-style gold as products of multiple overprinting mineralizing events during about 45 m.y. of deformation (e.g. Bateman et al., 2001), whereas others favour more-or-less synchronous gold deposition during progressive deformation of a package of rheologically variable rocks relatively late in the deformation history (Vielreicher et al., 2010).

Most agree that gold mineralization was post-peak regional metamorphism but the structural timing of the Fimiston lodes is disputed. Some workers conclude that the lodes formed early (pre to early D1) as they are supposedly cut by all structures in the deposit area including the gentle west-dipping D2 thrusts that locally host bonanza Green-Leader, or Oroya-style, lodes (e.g. Wells, 1964; Bateman and Hagemann, 2004). However, structural analysis by the majority of workers conclude that Fimiston lodes clearly overprint D1 structures and, together with the Green Leader mineralization, evolved broadly synchronous with the regional NW-trending D2 foliation (e.g. Boulter et al., 1987; Mueller et al., 1988; Gauthier et al., 2004; Weinberg et al., 2005). Mueller et al.

(1988) surmised that the Fimiston lodes are related to D2 shearing as their orientations fit a Riedel-model, where the Main lodes are P- or D-shears, Caunter lodes are P′- or R-shears, Easterly lodes are R-shears, Cross lodes are tensional ("T") structures, and Green Leader shoots occur at lode intersections.

The Mt Charlotte-style stockworks are generally described as a network of fracture- and shear- veins within faulted blocks of rheologically-contrasting Unit 8 of the Golden Mile Dolerite or porphyry dykes within Hannans Lake Serpentinite, and are spatially associated with, or bound by steep- and gently-dipping fault sets that cut the regional D2, and are variably described as D3 or D4 and include reactivated earlier structures (Table 3; e.g. Clout, 1989; Scott, 1997; Ridley and Mengler, 2000; Weinberg et al., 2005; Mueller, 2015 and references therein). There are two main schools of thought: (1) the veins formed in response to movement on the bounding brittle faults or related aftershock activity (e.g. Scott, 1997; Bateman et al., 2001), and (2) the faults were not suitably orientated for movement during vein formation, but rather increased stresses within the rheologically stiff units during D4 led to rock failure and vein development (e.g. Ridley and Mengler, 2000). Either way, the Mt Charlotte-style veins are consistently described as structurally younger than the Fimiston-style lodes, although a model in which the D3 and D4 structures initially formed to accommodate D2 strain in the more brittle rocks cannot be excluded as the far-field stresses during D2 to D4 are essentially the same.

Problems in interpreting both the timing relationships between the gold lodes and the porphyry dykes that intrude the area, as well as zircon ages from the more mafic dykes, have fuelled the controversy on the timing of the Fimiston gold mineralization (see discussion in Vielreicher et al., 2010). All the post-volcanic dykes share similar orientations with the Fimiston lodes. However, the feldspar-phyric dykes are clearly overprinted by all styles of mineralization. The relationship between the hornblende-phyric dykes and gold mineralization is more ambiguous, and some dykes have been described as inter-mineral (e.g. Gauthier et al., 2004). The lamprophyre dykes intrude mineralized structures, but are themselves altered, and hence are considered to have intruded during Fimiston-style mineralization (Gauthier et al., 2004; McNaughton et al., 2005).

This giant ore system therefore formed after c. 2.69 Ga basic magmatism, emplacement of the Golden Mile Dolerite at c. 2.68 Ga, and deposition of volcano-sedimentary Black Flag Beds and coeval intrusion of feldspar-phyric porphyry dykes at c. 2.67 to 2.66 Ga (Fig. 6). Gold mineralization potentially overlapped the end of hornblende-phyric dyke emplacement between c. 2.66 Ga and 2.65 Ga, but was broadly coeval with lamprophyre dyke intrusion at c. 2.65 Ga to 2.64 Ga (Fig. 6). Gold mineralization was post-peak regional metamorphism, which is considered to have occurred prior to c. 2.65 Ga, consistent with petrographic studies of wallrock alteration.

Direct dating of ore-related, hydrothermal monazite and xenotime in ore samples from the structurally late, brittle Mt Charlotte deposit yield ages of 2655 ± 13 Ma (Rasmussen et al., 2009) and 2644 ± 11 Ma (Vielreicher et al., 2010), whereas the most precise data from the structurally older Fimiston-ore samples provide an age of 2632 ± 12 Ma (Vielreicher et al., 2010), and a minimum age of 2636 Ma for Oroya-mineralization (McNaughton et al., 2005). Published $^{40}Ar/^{39}Ar$ dates of 2641 ± 13 Ma and 2643 ± 13 Ma for hydrothermal, gold-related sericite from the Golden Mile (recalculated from Kent and McDougall, 1995 by Vielreicher et al., 2010; Table 3) overlap all these data. Hence, as geological evidence indicates that Mt Charlotte ore formed after the Fimiston ore, it must be concluded that both ore types must have formed within 10 m. y. of each other at around 2.64 Ga (i.e. defined by maximum age for Fimiston ore and the minimum age for Mt Charlotte ore formation; Fig. 6).

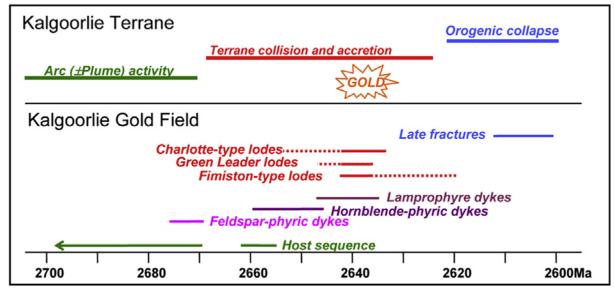

Figure 6. Timing of events in the Kalgoorlie Gold Field relative to regional tectonic events in the Kalgoorlie Terrane (as summarized in Vielreicher et al., 2015). The solid lines represent the interpreted timing of events based on geological relationships and geochronology. Dashed lines indicate the full range of geochronological data for gold samples. See text for further explanation.

A late chlorite-stable event overprints the Golden Mile and Mt Charlotte deposits and has been dated at 2603 ± 18 Ma (xenotime U-Pb; Vielreicher et al., 2010) and is coeval with published $^{40}Ar/^{39}Ar$ white mica data from the Golden Mile (Table 3). This event is coeval with events recorded at c. 2.61–2.60 Ga in most deposits in the Kalgoorlie Terrane (Vielreicher et al., 2015) and most probably records final terrane uplift, cooling and stabilization (Witt et al., 1996).

10. Genesis of the giant Kalgoorlie Gold Field

Many hypotheses have been proposed for the genesis of the giant accumulation of gold at Kalgoorlie Gold Field. They have variously been considered to be: (1) synvolcanic deposits associated with the overlying felsic volcanic sequence or felsic porphyry dykes (Gustafson and Miller, 1937; Travis et al., 1971; Clout, 1989); (2) modified syngenetic deposits (Tomich, 1974, 1976; Golding, 1978; Golding and Keays, 1981); or (3) epigenetic deposits temporally related to deformation, with ore fluids derived from metamorphism, magmatism or both (Campbell, 1953; Woodall, 1965; Golding, 1982; Boulter et al., 1987; Mueller et al., 1988). With an increased amount of ever more detailed studies over the last 30 or so years, the volume of data has greatly increased but the same arguments remain. Furthermore, differences in structural style, and particularly the different structural timing, has led some workers to propose different models for the Golden Mile and Mt Charlotte deposits. The main genetic models that are currently discussed are outlined below.

(1) The Golden Mile is a synvolcanic, epithermal gold-telluride deposit where hydrothermal activity is related to synvolcanic felsic magmatism, with fluids derived from either seawater or low- latitude meteoric water, and gold deposition resulted from fluid desulphidation during interaction with chemically-favourable wall rocks. Mt Charlotte, on the other hand, is described as more akin to other epigenetic lode-gold orogenic deposits that are associated with regional metamorphism and deformation (Clout, 1989; Clout et al., 1990);
(2) Both deposits are epigenetic, but formation was separated in time by a discrete deformation event (D3: Mueller, 2015). Both are related to episodic synorogenic calc-alkaline magmatism, with hydrothermal fluids at Mt Charlotte associated with the small volume of high-Mg monzodiorite porphyry dykes and a hypothetical intrusion buried 2 to 4 km down plunge from the deposit. Gold deposit formation is described as the product of

mainly wall-rock sulphidation, but fluid cooling is also interpreted to have played an important role at Mt Charlotte (Mueller et al., 1988; Mueller, 2015);

(3) The Fimiston lodes represent shallow-level epithermal-style gold-telluride mineralization that formed from deep crustal-derived, magmatic-metamorphic hydrothermal fluids that experienced phase immiscibility due to dramatic pressure fluctuations during repeated seismic events, and mixing with downward penetrating seawater. The Fimiston lodes were overprinted by both epigenetic epi- to meso-zonal gold veins (Green Leader) that formed from a magmatic fluid associated with a granite body buried beneath the deposit, and later mesozonal orogenic style veins (Mt Charlotte) that resulted from ascending, homogeneous, low-salinity fluids that also underwent phase immiscibility, fluid reaction and equilibration with interflow black shale units containing synsedimentary pyrite (Bateman and Hagemann, 2004);

(4) Both deposits formed in an epigenetic setting where gold deposit formation was purely the result of orogenic processes, with no significant direct involvement of local magmatic fluids, but rather a single, deeply-sourced, relatively homogeneous, mineralizing fluid that was sourced during regional metamorphism within the greenstone lithologies lower in the continental crust (e.g. Phillips and Powell, 2009) or from a subducting slab and its overlying sedimentary wedge (Goldfarb and Santosh, 2014; Groves and Santosh, 2016). Gold deposition was dominantly the result of continued wall-rock interaction and reaction, together with internal phase separation during cooling and pressure release.

Despite the differences in the two deposits, they have many characteristics in common (Table 3). They both comprise early shear-zone related gold-bearing pyrite-telluride mineralization (dominant in Golden Mile, but also present at Mt Charlotte), that is structurally overprinted by gold bearing pyrite/pyrrhotite vein stockworks (dominant at Mt Charlotte, but also present at the Golden Mile) that contain a significantly lower proportion of telluride minerals. Mineralogical, fluid inclusion and isotopic studies all support formation from a dominantly low-salinity, potassic H_2O-CO_2(+CH_4) fluid (or fluids), at similar temperature and pressure ranges through interaction and reaction with rheologically and chemically favourable wall rocks (Table 3). The presence of methane in the ore fluid has been attributed to mixing with an externally derived fluid, or to post-entrapment fluid modification (e.g. Hagemann and Brown, 1996; Mernagh et al., 2004). However, it could also be the product of fluid–rock interaction and reduction of juvenile carbon dioxide (Mikucki and Heinrich, 1993; Polito et al., 2001), which was generated during desulphidation of the ore fluid, that also caused destabilization of gold thiosulphide complexes and precipitation of pyrite and gold.

Furthermore, precise geochronology indicates that both styles of mineralization formed at roughly the same time, within about 10 m.y. of each other, around 2.64 Ga: that is, about 20–30 m.y. after the peak of intrusion of the feldspar-phyric porphyry dykes (c. 2.67 Ga) and after deposition of the Black Flag volcaniclastic-sedimentary rocks in the area (c. 2.69 to 2.655 Ga; Krapež et al., 2000). So, models that invoke a syn-volcanic timing for gold mineralization can now be ruled out. It is interesting to note that any inter-deposit compositional variation (e.g. $\delta^{34}S$ values) is either variable on an intra-deposit scale as well, or can be explained as the result of interaction with wall rocks or by local sources of metals (e.g. Pb). Such isotopic criteria have proved unreliable as a means to distinguish the two systems, or provide a definitive constraint on the source of the fluid and gold therein. However, the similarity in fluid characteristics, alteration and overall *P-T* conditions of mineralization is difficult to reconcile with a model where each deposit is the product of different mineralizing processes that operated at roughly the same time in roughly the same space. In contrast, it supports a model in which both ore styles are the product of a single complex system that operated after peak metamorphism in the surrounding wall rocks, and was coeval with late compressional to transpressional deformation (D2–D4) associated with terrane accretion. Therefore, although the gold mineralization is clearly orogenic in timing, the question remains as to whether this complex hydrothermal system formed from magmatic-hydrothermal or orogenic processes, as it also temporally overlaps intrusion of the volumetrically minor hornblende-phyric (Mg-monzodiorite) and lamprophyric dykes, which occupy similar structural sites to the gold mineralization in the Golden Mile (e.g. Mueller et al., 1988).

The systematics at the site of gold deposition, and how the gold-bearing fluid interacted with the host rocks to produce a gold deposit are well described at Kalgoorlie. It is known that the system operated on a kilometre scale (at least), next to an active crustal-scale fault system that accommodated rapid uplift and erosion of several kilometres of strata before deposition of volcanic and clastic sedimentary basinal rocks. These faults also provided an extremely efficient plumbing system for magmas, including lithosphere-derived lamprophyres, and hydrothermal fluids from the deep crust/lithosphere to reach the interconnected mesh of upper crustal structures in an uplifted block (inlier) of ultramafic to mafic greenstone rocks within the giant Gold Field. The syn-deformation, syn-accretion, structural control on mineralization is also well described as is its late timing relative to regional metamorphism of adjacent host rocks. Ore fluids consisted of an originally reduced, low-salinity, CO_2-bearing, ^{18}O enriched fluid, that interacted with wall rocks along its path, which caused localized modifications in its isotopic composition and deposited gold due to reaction with chemically favourable rocks, together with decreases in solubility of gold complexes during declining temperature and rapid pressure releases. As such, it is a typical example of an orogenic deposit formed from a fluid that was sourced deep within or beneath the supracrustal rocks, and/or from devolatilization of the subducting slab and overlying sulphidic oceanic sediment wedge, during accretionary tectonism.

Another important factor to consider is the relationship of the Kalgoorlie Gold Field relative to other deposits in the Terrane and indeed the Province. A regional geochronological study showed that the period of gold deposition at Kalgoorlie overlaps that of gold deposition at all other dated deposits in the Kalgoorlie Terrane, but is about 10 m.y. younger than deposits in the neighbouring Kurnalpi Terrane to the east (Vielreicher et al., 2015). This is consistent with other stratigraphic, magmatic and structural trends that show a westward younging direction related to progressive westward-directed accretion of the Terranes of the eastern Yilgarn to the Proto-Yilgarn in the west. As such, gold mineralization must be considered a consequence of these crustal-scale tectonic processes.

11. The conjunction of factors that make Kalgoorlie a giant gold field

Groves et al. (2016), following earlier authors such as Phillips et al. (1996), discuss the critical conjunction of factors required to form a giant gold field and/or a giant gold deposit. Those factors that appear important specifically for the giant Kalgoorlie Gold Field and the giant to supergiant Golden Mile deposit are outlined briefly below.

At the tectonic scale, Kalgoorlie lies close to a major lithospheric boundary separating the Kalgoorlie Terrane with young (c. 2.7 Ga) lithosphere to the east from older (>3.0 Ga) lithosphere to the west

(Fig. 2; Mole et al., 2013; McCuaig and Hronsky, 2014). Such boundaries, particularly associated with deeply penetrating faults, appear important for the generation of a variety of giant gold and gold-copper deposits (Groves and Santosh, 2015; Groves et al., 2016). The crustal-scale Boulder-Lefroy Fault, adjacent to the Kalgoorlie Gold Field is such a deeply-penetrating fault that has played a role in focussing auriferous ore fluids to form a number of world-class gold fields along its length: from south to north; Norseman, Kambalda-St Ives, New Celebration, Kalgoorlie, Kanowna and Paddington. Collectively, these deposits have produced about 50% of Yilgarn gold, attesting to the importance of the Boulder-Lefroy Fault. In terms of age, the host greenstone belt at Kalgoorlie is c 2.7 Ga, the time of one of the greatest orogenic gold-forming episodes in Earth history (e.g., Goldfarb et al., 2001). The Kalgoorlie Gold Field also sits within a zone of arguably the most complex structural geometry in the Kalgoorlie Terrane. This has been caused by superimposition of D1 to D4 structures to form a folded thrust-lithostratigraphic package adjacent to a NW-trending dilational jog in the regionally NNW-trending Boulder-Lefroy Fault. D1 thrusting followed by D2 upright folding has produced a large anticlinal structure, a key component of most giant orogenic gold systems, which has isolated a relatively brittle mafic sequence, including the Golden Mile Dolerite, within a relatively incompetent and impermeable envelope of Black Flag sedimentary rocks. This is a perfect scenario for selective failure of the competent mafic rocks, particularly the thick Golden Mile dolerite, during deformation and synchronous seismic pumping of auriferous fluid into the lithostratigraphic package, while the overlying sedimentary rocks served as an aquaclude to cap the hydrothermal system. Within this overall favourable system, early thrust-repetition of the Golden Mile Dolerite at the site of the Golden Mile deposit almost certainly doubled the volume of competent rock for selective failure and hence promoted the formation of a giant deposit in that locality. Broadly NE-trending fault networks, normally attributed to D3 or D4, could have initially formed as accommodation structures in brittle rocks that could not accommodate brittle-ductile strain during D2 compression, and certainly controlled the extent of stockwork gold mineralization at Mt Charlotte. Similarly, the gold lodes at the Golden Mile are bounded to the north by the NE-trending Golden Pike Fault and to the south by the similarly oriented Adelaide Fault, suggesting these played a key role in focussing the fluid to form the giant deposit. Finally, the whole Kalgoorlie Gold Field lithostratigrahic package has been uplifted relative to surrounding blocks which include the late Merougil Beds to the west (e.g., Tripp, 2014). Reduction in lithostatic pressure would have aided phase separation of ore fluids during seismic events, further enhancing gold deposition, as initially suggested by Groves et al. (1987).

Hence, the giant Kalgoorlie Gold Field was formed by a fortuitous conjunction of highly favourable parameters, with the Golden Mile located in the most favourable structural position where there was duplication of a competent block of Golden Mile Dolerite in a locked-up NW-trending anticlinal hinge segmented by NE-trending cross faults. In all prospectivity mapping studies, using a variety of derived critical parameters and a variety of methodologies to combine them, the Kalgoorlie Gold Field inevitably stands out as the only district where all parameters were in alignment, as summarized by Groves et al. (2000).

12. Concluding statement

The Kalgoorlie Gold Field comprises two dominant ore types, both of which are consistent with deposition from a juvenile, potassic, low salinity, CO_2 ($\pm CH_4$) bearing aqueous fluid that both phase separated and inter-reacted with wall rocks to form gold and associated sulphide and telluride mineral assemblages. Geochronology supports both styles having been deposited within 10 m. y. of each other (the limit of precision of U-Pb and Ar-Ar ages) around 2.64 Ga. The exact source of the fluid remains speculative but current constraints on the fluid composition, including fluid inclusion, stable and radiogenic isotope compositions, are consistent with a metamorphic fluid that was derived from deeper parts of the volcanic supracrustal sequences, or even deeper and reacted with crustal rocks along crustal-scale faults or shear zones that controlled regional fluid pathways. Alternatively, the fluids and gold could have been derived from devolatilization of the subducting slab and overlying sulphidic sedimentary wedge during accretion of the Kalgoorlie Terrane to the Youanmi Terrane of the Proto-Yilgarn. The Kalgoorlie Gold Field is one of the world's largest gold fields, with the Golden Mile approaching supergiant status, because there is a conjunction of all the critical features required to form a giant orogenic gold district: close proximity to a auriferous fluid-focussing crustal-scale fault; complex geometry related to overprinting deformation events; a major locked-up anticline in an uplifted block; thick, competent, iron-rich reactive host-rocks, duplicated in thickness by thrusting at the Golden Mile, surrounded by incompetent sedimentary sequences that capped the hydrothermal system, and cross faults that compartmentalized ore fluid flux into the competent units.

Acknowledgements

Most of the research carried out by NMV on the eastern Goldfields Province of the Yilgarn Craton was as an ARC Linkage- and AMIRA P680-funded postdoctoral research fellow at the Centre for Global Metallogeny, now the Centre for Exploration Targeting, at the University of Western Australia (UWA). Contributions by DIG and NJMcN are based on the culmination of over 30 years independent research and collaborative work with others in the gold research group at UWA, and with Dr. Rich Goldfarb of USGS and late Prof. Rob Kerrich of the University of Saskatchewan. Dr Richard Vielreicher is also thanked for his encouragement and proof reading skills despite extremely difficult personal circumstances. Two anonymous reviewers and Prof. Santosh from the GSF Editorial Board are thanked for comments on an earlier draft of this manuscript.

References

Barley, M.E., Eisenlohr, B.N., Groves, D.I., Perring, C.S., Vearncombe, J.R., 1989. Late Archean convergent margin tectonics and gold mineralization; a new look at the Norseman-Wiluna Belt, Western Australia. Geology 17, 826–829.

Barley, M.E., Brown, S.J.A., Krapež, B., Kositcin, N., 2008. Physical volcanology and geochemistry of a late Archaean volcanic arc: Kurnalpi and Gindalbie Terranes, Eastern Goldfields Superterrane, Western Australia. Precambrian Research 161, 53–76.

Bartram, G.D., 1969. Wall-rock alteration associated with auriferous lodes at Kalgoorlie. PhD Thesis. The University of Western Australlia, 396 p.

Bateman, R.J., Hagemann, S.G., 2004. Gold mineralisation throughout about 45 Ma of Archaean orogenesis: protracted flux of gold in the Golden Mile, Yilgarn craton, Western Australia. Mineralium Deposita 39, 536–559.

Bateman, R.J., Hagemann, S.G., McCuaig, T.C., Swager, C.P., 2001. Protracted Gold Mineralization throughout Archean Orogenesis in the Kalgoorlie Camp, Yilgarn Craton, Western Australia: Structural, Mineralogical, and Geochemical Evolution. Geological Survey of Western Australia Record 2001/17, pp. 63–98.

Blainey, G., 1993. The Golden Mile: Australia. Allen and Unwin, p. 184.

Blewett, R.S., Czarnota, K., Henson, P.A., 2010. Structural-event framework for the eastern Yilgarn Craton, Western Australia, and its implications for orogenic gold. Precambrian Research 183, 203–229.

Boulter, C.A., Fotios, M.G., Phillips, G.N., 1987. The Golden Mile, Kalgoorlie: a giant gold deposit localized in ductile shear zones by structurally induced infiltration of auriferous metamorphic fluids. Economic Geology 82, 1661–1678.

Brown, S.J.A., Barley, M.E., Krapež, B., Hand, J., Cas, R.A.F., 2001. The origin of TTD volcaniclastic rocks in the Kalgoorlie Terrane, Western Australia. Australian Geological Survey Organisation -Geoscience Australia Record 37, 131–133.

Cabri, L.J., 1965. Phase relations in the Au–Ag–Te system and their mineralogical significance. Economic Geology 60, 1569–1606.

Cameron, E.M., 1988. Archean gold: relation to granulite formation and redox mixing in the crust. Geology 16, 109–112.

Campbell, J.D., 1953. The structure of the Kalgoorlie Gold field. In: Edwards, A.B. (Ed.), Geology of Australian Ore Deposits. Australasian Institute of Mining and Metallurgy, pp. 79–93.

Card, G.W., 1898. Notes on the country rock of the Kalgoolie Goldfield. Geological Survey of New South Wales Record 6, 17–42.

Champion, D.C., Sheraton, J.W., 1997. Geochemistry and Nd isotope systematics of Archaean granites of the Eastern Goldfields, Yilgarn Craton, Australia; implications for crustal growth processes. Precambrian Research 83, 109–132.

Claoue-Long, J.C., Compston, W., Cowden, A., 1988. The age of the Kambalda greenstones resolved by ion-microprobe: implications for Archaean dating methods. Earth and Planetary Science Letters 89, 239–259.

Clark, M.E., 1980. Localization of Gold, Mt Charlotte, Kalgoorlie, Western Australia. BSc Honours thesis. University of Western Australia.

Clout, J.M.F., 1989. Structural and Isotopic Studies of the Golden Mile Gold-telluride Deposit, Kalgoorlie, W. A. Unpublished PhD thesis. Monash University.

Clout, J.M.F., Cleghorn, J.H., Eaton, P.C., 1990. Geology of the Kalgoorlie Goldfield. Australiasian Institute of Mining and Metallurgy Monograph 14, 411–431.

Colvine, A.C., Fyon, J.A., Heather, K.B., Marmont, S., Smith, P.M., Troop, D.G., 1988. Archaean Lode Gold Deposits in Ontario. Ontario Geological Society Miscellaneous Paper 139, p. 136.

Czarnota, K., Blewett, R., Champion, D.C., Henson, P.A., Cassidy, K.F., 2007. Significance of extensional tectonics in orogenic gold systems: an example from the Eastern Goldfields Superterrane, Yilgarn Craton, Australia. In: Andrew, C.L., et al. (Eds.), Digging Deeper. Proceedings of the Ninth Biennial Meeting of the Society for Geology Applied to Mineral Deposits, vol. 2, pp. 1431–1434.

Czarnota, K., Blewett, R.S., Goscombe, B., 2010. Predictive mineral discovery in the eastern Yilgarn Craton, Western Australia: an example of district scale targeting of an orogenic gold mineral system. Precambrian Research 183, 356–377.

Dahl, N., McNaughton, N.J., Groves, D.I., 1987. A lead-isotope study of sulphides associated with gold mineralization in selected gold deposits from the Eastern Goldfields of Western Australia. In: Ho, S.E., Groves, D.I. (Eds.), Recent Advances in Understanding Precambrian Gold Deposits, pp. 189–201. University of Western Australia, Geology Department (Key Centre) and University Extension Publication 11.

Frecheville, W.M., 1898. Notes to a visit to the gold mines at Kalgoorlie, Western Australia. Transactions of the Institute of Mining and Metallurgy 6, 140–152.

Gauthier, L., Hagemann, S.G., Robert, F., Pickens, G., 2004. New constraints on the architecture and timing of the giant Golden Mile gold deposit, Kalgoorlie, Western Australia. In: Groves, D.I. (Ed.), SEG2004: Predictive Mineral Discovery under Cover, Extended Abstracts. Society of Economic Geologists, Conference Series, pp. 353–356.

Goldfarb, R.J., Santosh, M., 2014. The dilemma of the Jiaodong gold deposits: are they unique? Geoscience Frontiers 5, 139–153.

Goldfarb, R.F., Groves, D.I., Gardoll, S., 2001. Orogenic gold and geologic time: a global synthesis. Ore Geology Reviews 18, 1–75.

Goldfarb, R.J., Baker, T., Dubé, B., Groves, D.I., Hart, C.J.R., Robert, F., Gosselin, P., 2005. World Distribution, Productivity, Character, and Genesis of Gold Deposits in Metamorphic Terranes. Economic Geology 100th Anniversary Volume, pp. 407–450.

Golding, L.Y., 1978. Mineralogy, Geochemistry and Origin of the Kalgoorlie Gold Deposit, Kalgoorlie. Unpublished PhD thesis. Melbourne University.

Golding, S.D., 1982. An Isotopic and Geochemical Study of Gold Mineralization in the Kalgoorlie-Norseman Region, Western Australia. PhD thesis. University of Queensland.

Golding, L.Y., Keays, R.R., 1981. Problems of ore genesis at Kalgoorlie. In: Sediments through the Ages, Fifth Australian Geological Convention, Perth, p. 70. Geological Society of Australia Abstracts 3.

Golding, S.D., Groves, D.I., McNaughton, N.J., Barley, M.E., Rock, N.M.S., 1987. Carbon isotopic compositions of carbonates from contrasting alteration styles in supracrustal rocks of the Norseman-Wiluna belt, Yilgarn Block, Western Australia: their significance to the source of Archaean auriferous fluids. In: Ho, S.E., Groves, D.I. (Eds.), Recent Advances in Understanding Precambrian Gold Deposits, pp. 215–238. University of Western Australia, Geology Department (Key Centre) and University Extension Publication 11.

Golding, S.D., Barley, M.E., Cassidy, K.F., Groves, D.I., Ho, S.E., Hronsky, J.M.A., McNaughton, N.J., Sang, J.H., Turner, J.V., 1990a. Constraints on genesis of primary gold deposits. In: Ho, S.E., Groves, D.I., Bennett, J. (Eds.), Gold Deposits of the Archaean Yilgarn Block, Western Australia: Nature, Genesis and Exploration Guides, pp. 252–258. University of Western Australia, Geology Department (Key Centre) and University Extension Publication 20.

Golding, S.D., Clark, M.E., Keele, R.A., Wilson, A.F., Keays, R.R., 1990b. Geochemistry of Archaean epigenetic gold deposits in the Eastern Goldfields Province, Western Australia. In: Herbert, H.K., Ho, S.E. (Eds.), Stable Isotopes and Fluid Processes in Mineralization, pp. 141–176. University of Western Australia, Geology Department (Key Centre) and University Extension Publication 23.

Golding, S.D., Groves, D.I., McNaughton, N.J., Mikucki, E.J., Sang, J.H., 1990c. Constraints on genesis of primary gold deposits. Gold deposits of the Archean Yilgarn Block, Western Australia: nature, genesis and exploration. In: Ho, S.E., Groves, D.I., Bennett, J. (Eds.), Gold Deposits of the Archaean Yilgarn Block, Western Australia: Nature, Genesis and Exploration Guides, pp. 259–262. University of Western Australia, Geology Department (Key Centre) and University Extension Publication 20.

Groves, D.I., Santosh, M., 2015. Province-scale commonalities of some world-class gold deposits: Implications for mineral exploration. Geoscience Frontiers 6, 389–399.

Groves, D.I., Santosh, M., 2016. The giant Jiaodong gold province: the key to a unified model for orogenic gold deposits? Geoscience Frontiers 7 (3), 409–417.

Groves, D.I., Phillips, G.N., Ho, S.E., Houstoun, S.M., Standing, C.A., 1987. Craton-scale distribution of Archaean greenstone gold deposits: predictive capacity of the metamorphic model. Economic Geology 82, 2045–2058.

Groves, D.I., Goldfarb, R.J., Knox-Robinson, C.M., Ojala, J., Gardoll, S., Yun, G.Y., Holyland, P., 2000. Late-kinematic timing of orogenic gold deposits and significance for computer- based exploration techniques with emphasis on the Yilgarn Block, Western Australia. Ore Geology Reviews 17, 1–38.

Groves, D.I., Goldfarb, R.J., Santosh, M., 2016. The conjunction of factors that lead to formation of giant gold provinces and deposits in non-arc settings. Geoscience Frontiers 7 (3), 303–314.

Gustafson, J.K., Miller, F.S., 1937. Kalgoorlie geology reinterpreted. Australian Institute Mining and Metallurgy Proceedings 106, 93–125.

Hagemann, S.G., Brown, P.E., 1996. Geobarometry in Archean lode-gold deposits. European Journal of Mineralogy 8, 937–960.

Hagemann, S.G., Bateman, R.J., Crowe, D., Vielreicher, R., 1999. In situ sulfur isotope composition of pyrites from the Fimiston- and Oroya-style gold lodes in the Golden Mile camp, Kalgoorlie. Geological Society of America Annual Conference Abstracts 31, A-245.

Hand, J.L., 1998. The Sedimentological and Stratigraphic Evolution of the Archaean Black Flag Beds, Kalgoorlie, Western Australia: Implications for Regional Stratigraphy and Basin Setting of the Kalgoorlie Terrane. Unpublished Ph.D. thesis. Monash University, Melbourne.

Heath, C.J., 2003. Fluid Flow at the Giant Golden Mile Deposit, Kalgoorlie, Western Australia. Unpublished PhD thesis. Australian National University, p. 173.

Ho, S.E., 1987. Fluid inclusions: their potential as an exploration tool for Archean gold deposits. In: Ho, S.E., Groves, D.I (Eds.), Recent Advances in Understanding Precambrian Gold Deposits, pp. 239–263. University of Western Australia, Geology Department (Key Centre) and University Extension Publication 11.

Ho, S.E., Bennett, J.M., Cassidy, K.F., Hronsky, J.M.A., Mikucki, E.J., Sang, J.H., 1990. Nature of ore fluid, and transportational and depositional conditions in sub-amphibolite facies deposits. In: Ho, S.E., Groves, D.I., Bennett, J. (Eds.), Gold Deposits of the Archaean Yilgarn Block, Western Australia: Nature, Genesis and Exploration Guides, pp. 198–211. University of Western Australia, Geology Department (Key Centre) and University Extension Publication 20.

Hunter, W.M., 1993. Geology of the Granite-greenstone Terrain of the Kalgoorlie and Yilmia 1:100,000 Sheets, Western Australia. Geological Survey of Western Australia Record 35.

Kent, A.J.R., McDougall, I., 1995. $^{40}Ar/^{39}Ar$ and U–Pb age constraints on the timing of gold mineralization in the Kalgoorlie gold field. Economic Geology 90, 845–859.

Kent, A.J.R., McDougall, I., McCullough, M.T., 1995. Sm-Nd systematics of hydrothermal scheelite from the Mount Charlotte mine, Kalgoorlie, Western Australia: an isotope link between gold mineralization and komatiites. Economic Geology 90, 2329–2335.

Krapež, B., 1997. Sequence-stratigraphic concepts applied to the identification of depositional basins and global tectonic cycles. Australian Journal of Earth Sciences 44, 1–36.

Krapež, B., Barley, M.E., 2008. Late Archaean synorogenic basins of the Eastern Goldfields Superterrane, Yilgarn Craton, Western Australia Part III. Signatures of tectonic escape in an arc-continent collision zone. Precambrian Research 161, 183–199.

Krapež, B., Hand, J.L., 2008. Late Archaean deep-marine volcaniclastic sedimentation in an arc-related basin: the Kalgoorlie sequence of the Eastern Goldfields Superterrane, Yilgarn Craton, Western Australia. Precambrian Research 161, 89–113.

Krapež, B., Brown, S.J.A., Hand, J.L., Barley, M.E., Cas, R.A.F., 2000. Age constraints on recycled crustal and supracrustal sources of Archaean metasedimentary sequences, Eastern Goldfields Province, Western Australia: evidence from SHRIMP zircon dating. Tectonophysics 322, 89–133.

Lambert, I.B., Phillips, G.N., Groves, D.I., 1984. Sulfur isotope compositions and genesis of Archean gold mineralization. In: Foster, R.P. (Ed.), Australia and Zimbabwe. Gold '82. A.A. Balkema Publication, pp. 373–388.

Larcombe, C.O.G., 1912. The geology of Kalgoorlie. Australasian Institute of Mining Engineering Transactions 14, 1–327.

Maitland, A.G., Campbell, W.D., 1902. Geological Map of Kalgoorlie, Western Australia. 10 Chains to 1 Inch Map. Geological Society of Western Australia, Perth.

McCuaig, T.C., Hronsky, J.M.A., 2014. The mineral system concept: the key to exploration targeting. Society of Economic Geologists Special Publication 18, pp. 153–175.

McLaren, M., 1910. The Kalgoorlie Goldfield. Unpublished report. Kalgoorlie Mining Associates.

McNaughton, N.J., Cassidy, K.F., Dahl, N., de Laeter, J.R., Golding, S.D., Groves, D.I., Ho, S.E., Mueller, A.G., Perring, C.S., Sang, J.H., Turner, J.V., 1992. The source of ore components in lode-gold deposits of the Yilgarn Block, Western Australia. In: Glover, J.E., Ho, S.E. (Eds.), The Archaean; Terrains, Processes and Metallogeny. Proceedings Volume for the Third International Archaean Symposium, pp. 351–363. University of Western Australia, Geology Department and Extension Services, Publication 22.

McNaughton, N.J., Mueller, A.G., Groves, D.I., 2005. The age of the giant Golden Mile Deposit, Kalgoorlie, Western Australia: ion-microprobe zircon and monazite U-Pb geochronology of a syn-mineralization lamprophyre dyke. Economic Geology 100, 1427–1440.
Mernagh, T.P., 1996. Gold Mineralisation at Mount Charlotte: Evidence for Fluid Oxidation from Fluid Inclusions, p. 292. Geological Society of Australia Abstracts 41.
Mernagh, T.P., Heinrich, C.A., Mikucki, E.J., 2004. Temperature gradients recorded by fluid inclusions and hydrothermal alteration at the Mount Charlotte gold deposit, Kalgoorlie, Australia. Canadian Mineralogist 42, 1383–1403.
Mikucki, E.J., Heinrich, C.A., 1993. Vein- and Mine-scale Wall-rock Alteration and Gold Mineralization in the Archean Mount Charlotte Deposit, Kalgoorlie, Western Australia. Kalgoolie '93 Extended Abstracts, Australian Geological Survey Organisation Record 1993/54, pp. 135–140.
Mikucki, J.E., Roberts, F.I., 2003. Metamorphic Petrography of the Kalgoorlie Region, Eastern Goldfields Granite-greenstone Terrane. MetPet database. Geological Survey of Western Australia, p. 40.
Mole, D.R., Fiorentini, M.L., Cassidy, K.F., Kirkland, C.L., Thebaud, N., McCuaig, T.C., Miller, J., 2013. Crustal evolution, intra-cratonic architecture and the metallogeny of an Archaean Craton. Geological Society, London, Special Publication 393, SP393–SP398. http://dx.doi.org/10.1144/SP393.8.
Morris, P.A., 1993. Archean Mafic and Ultramafic Volcanic Rocks, Menzies to Norseman, Western Australia, p. 107. Western Australian Geological Survey Report 36.
Mueller, A.G., 2007. Copper-gold endoskarns and high-Mg monzodiorite-tonalite intrusions at Mt Shea, Kalgoorlie, Australia: implications for the origin of gold-pyrite-tennantite mineralization in the Golden Mile. Mineralium Deposita 42, 737–769.
Mueller, A.G., 2015. Structure, alteration, and geochemistry of the Charlotte quartz vein stockwork, Mt Charlotte gold mine, Kalgoorlie, Australia: time constraints, down-plunge zonation, and fluid source. Mineralium Deposita 50, 221–244. http://dx.doi.org/10.1007/s00126-014-0527-2.
Mueller, A.G., Harris, L.B., Lungan, A., 1988. Structural control on greenstone-hosted gold mineralization by transcurrent shearing: a new interpretation of the Kalgoorlie mining district, Western Australia. Ore Geology Reviews 3, 359–387.
Mueller, A.G., de Laeter, J.R., Groves, D.I., 1991. Strontium isotope systematics of the hydrothermal minerals from epigenetic Archean gold deposits in the Yilgarn Block, Western Australia. Economic Geology 86, 780–809.
Mueller, A.G., Muhling, J.R., 2013. Silver-rich telluride mineralization at Mount Charlotte and Au-Ag zonation in the giant Golden Mile deposit, Kalgoorlie, Western Australia. Mineralium Deposita 48, 295–311. http://dx.doi.org/10.1007/s00126-012-0425-4.
Neall, F.B., 1987. Sulphidation of iron-rich rocks as a precipitation mechanism for large Archaean gold deposits in Western Australia: thermodynamic confirmation. In: Ho, S.E., Groves, D.I. (Eds.), Recent Advances in Understanding Precambrian Gold Deposits, pp. 265–269. University of Western Australia, Geology Department (Key Centre) and University Extension Publication 11.
Nixon, D., Hesford, C., Fotzgerald, M., Lister, G., 2014. Relative Timing of Gold Mineralisation within the Kalgoorlie Camp. Gold14@Kalgoorlie International Symposium Extended Abstracts. Australian Institute of Geoscientists, pp. 97–98.
O'Beirne, W.R., 1968. The Acid Porphyries and Porphyroid Rocks of the Kalgoorlie Area. Unpublished PhD thesis. The University of Western Australia, p. 410.
Perring, C.S., Groves, D.I., Shellabear, J.N., Hallberg, J.A., 1991. The "porphyry-gold" association in the Norseman-Wiluna Belt of Western Australia: implications for models of Archaean gold metallogeny. Precambrian Research 51, 85–113.
Phillips, G.N., 1986. Geology and alteration in the Golden Mile Kalgoorlie. Economic Geology 81, 779–808.
Phillips, G.N., Powell, R., 2009. Formation of gold deposits: review and evaluation of the continuum model. Earth-Science Reviews 94, 1–21.
Phillips, G.N., Groves, D.I., Amaro, D., Hallbauer, D.K., Fotios, M.G., 1988. Morphology and trace-element compositions of pyrites from Kalgoorlie gold deposits: sensitive indicators of syn -deformational fluid regimes and depositional indicators of syn -deformational fluid regimes and depositional processes. In: Ho, S.E., Groves, D.I. (Eds.), Advances in understanding Precambrian gold deposits, vol. II, pp. 217–226. University of Western Australia. Geology Department (Key Centre) and University Extension Publication 12.
Phillips, G.N., Groves, D.I., Kerrich, R., 1996. Factors in the formation of the giant Kalgoorlie gold deposit. Ore Geology Reviews 10, 295–317.
Phillips, N.G., Gibb, H.F.C., 1993. A century of mining at Kalgoorlie. Economic Geology Research Unit, Key Centre in Economic Geology, James Cooke University of North Queensland. Contribution 45.
Polito, P.A., Bone, Y., Clarke, J.D.A., Mernagh, T.P., 2001. Compositional zoning of fluid inclusions in the Archaean Junction gold deposit, Western Australia: a process of fluid-wall-rock interaction? Australian Journal of Earth Sciences 48, 833–855.
Rasmussen, B., Mueller, A.G., Fletcher, I.R., 2009. Zirconolite and xenotime U-Pb age constraints on the emplacement of the Golden Mile dolerite sill and gold mineralization at the Mount Charlotte mine, Eastern Goldfields Province, Yilgarn craton, Western Australia. Contributions to Mineralogy and Petrology 157, 559–572.
Ridley, J.R., Mengler, F., 2000. Lithological and structural controls on the form and setting of vein stockwork ore bodies at the Mt Charlotte gold deposit, Kalgoorlie. Economic Geology 95, 85–98.
Robert, F., 2001. Syenite-associated disseminated gold deposits in the Abitibi greenstone belt, Canada. Mineralium Deposita 36, 503–516.
Robert, F., Poulson, H.K., Cassidy, K.F., Hodgson, J.C., 2005. Gold Metallogeny of the Superior and Yilgarn Cratons. Economic Geology 100th Anniversary Volume, pp. 1001–1033.
Scantlebury, G.M., 1983. The Characteristics and Origin of Gold Lodes in and Around the Brownhill Syncline, Golden Mile, Kalgoorlie, Western Australia. Unpublished BSc (Honours) thesis. University of Western Australia, p. 103.
Scott, R.J., 1997. Fault control on fluid flow and mineralization at Mount Charlotte and the Golden Mile. Kalgoorlie '97, an International Conference on the Crustal Evolution, Metallogeny and exploration of the Yilgarn block – an update. In: Cassidy, K.F., Whitaker, A.J., Liu, S.F. (Eds.), Australian Geological Survey Organisation Record 1997/41, pp. 169–174.
Shackleton, J.M., Spry, P.G., Bateman, R., 2003. Telluride mineralogy of the golden mile deposit, Kalgoorlie, Western Australia. Canadian Mineralogist 41, 1503–1524.
Steadman, J.A., Large, R.R., Meffre, S., Olin, P.H., Danyushevsky, L.V., Gregory, D.D., Belousov, I., Lounejava, E., Ireland, T., Holden, P., 2015. Synsedimentary to early diagenetic gold in black shale-hosted pyrite nodules at the Golden Mile Deposit, Kalgoorlie, Western Australia. Economic Geology 110, 1157–1191.
Stillwell, F.L., 1929. Geology and ore deposits of the Boulder belt, Kalgoorlie. Geological Survey of Western Australia Bulletin 94, 1–110.
Swager, C.P., 1989. Structure of Kalgoorlie Greenstones – Regional Deformation History and Implications for the Structural Setting of the Golden Mile Gold Deposits, pp. 59–84. Geological Survey of Western Australia Report 25.
Swager, C.P., 1997. Tectono-stratigraphy of Late Archaean greenstone terranes in the southern Eastern Goldfields, Western Australia. Precambrian Research 83, 11–42.
Swager, C.P., Witt, W.K., Griffin, T.J., Ahmat, A.L., Hunter, W.M., McGoldrick, P.J., Wyche, S., 1992. Late Archaean granite-greenstones of the Kalgoorlie Terrane, Yilgarn Craton, Western Australia. In: Glover, J.E., Ho, S.E. (Eds.), The Archaean; Terrains, Processes and Metallogeny. Proceedings Volume for the Third International Archaean Symposium, pp. 107–122. University of Western Australia, Geology Department and Extension Services, Publication 22.
Swager, C.P., Griffin, T.J., Witt, W.K., Wyche, S., Ahmat, A.L., Hunter, W.M., McGoldrick, P.J., 1995. Geology of the Archaean Kalgoorlie Terrane—an Explanatory Note, p. 26. Geological Survey of Western Australia Report 48.
Tomich, S.A., 1974. A new look at Kalgoorlie Golden Mile geology. Australasian Institute of Mining and Metallurgy Proceedings 251, 27–35.
Tomich, S.A., 1976. Further thoughts on the application of the volcanogenic theory to the Golden Mile ores at Kalgoorlie. Australiasian Institute of Mining and Metallurgy Proceedings 258, 19–29.
Travis, G.A., Woodall, R., Bartram, G.D., 1971. The Geology of the Kalgoorlie Goldfield, pp. 175–190. Geological Society of Australia Special Publication 3.
Tripp, G., 2014. How Neoarchean stratigraphy and structural geology determine the timing and controls of world-class greenstone gold camps in the Eastern Goldfields Province: key factors for gold exploration. Gold'14 extended abstracts. Australian Institute of Geoscientists Bulletin 59, 124–128.
Turek, A., Compston, W., 1971. Rubidium-strontium Geochronology in the Kalgoorlie Region, p. 72. Geolological Society of Australia Special Publication 3.
Vielreicher, N.M., Groves, D.I., Snee, L.W., Fletcher, I.R., McNaughton, N.J., 2010. Broad synchroneity of three gold mineralization styles in the Kalgoorlie Gold Field: SHRIMP U-Pb and Ar/Ar geochronological evidence. Economic Geology 105, 187–227.
Vielreicher, N.M., Groves, D.I., McNaughton, N.J., 2015. The timing of gold mineralization across the eastern Yilgarn craton using U–Pb geochronology of hydrothermal phosphate minerals. Mineralium Deposita 50, 391–428.
Weinberg, R.F., van der Borgh, P., 2008. Extension and gold mineralization in the Archean Kalgoorlie terrane, Yilgarn craton. Precambrian Research 161, 77–88.
Weinberg, R.F., Moresi, L., van der Borgh, P., 2003. Timing of deformation in the Norseman-Wiluna Belt, Yilgarn craton, Western Australia. Precambrian Research 120, 219–239.
Weinberg, R.F., van der Borgh, P., Bateman, R.J., Groves, D.I., 2005. Kinematic history of the Boulder-Lefroy shear zone system and controls on associated gold mineralization, Yilgarn Craton, Western Australia. Economic Geology 100, 1407–1426.
Weller, K.R., Campbell, J.J., Thornber, M.R., Wilkie, G.J., Bateman, R., Ellis, S., 1998. A coherent metallurgical testing and particle characterization for mine planning, process flow sheet development, and downstream problem identification. In: Australasian Institute of Mining and Metallurgy Annual Conference '98, Mt Isa. The Mining Cycle.
Wells, A.A., 1964. Western lode structures and southward extensions of the Boulder mining belt. Proceedings of the Australasian Institute of Mining and Metallurgy 211, 181–192.
White, R.W., Rowell, R., Phillips, G.N., 2003. A mineral equilibria study of the hydrothermal alteration in mafic greenschist facies rocks at Kalgoorlie, Western Australia. Journal of Metamorphic Geology 21, 455–468.
Witt, W.K., Swager, C.P., Nelson, D.R., 1996. ^{40}Ar-^{39}Ar and U–Pb age constraints on the timing of gold mineralization in the Kalgoorlie Gold Fields, Western Australia – a discussion. Economic Geology 91, 1354–1371.
Woodall, R.W., 1965. Structure of the Kalgoorlie Goldfield. In: McAndrew, J. (Ed.), Geology of Australian Ore Deposits. 8th Commonwealth Mining and Metallurgy Congress, Melbourne, pp. 71–79.
Woods, B.K., 1997. Petrogenesis and Geochronology of Felsic Dykes in the Kalgoorlie Terrane, Kalgoorlie, Western Australia. Unpublished BSc (Honours) thesis. Curtin University of Technology, Perth, p. 108.
Yeats, C.J., McNaughton, N.J., Ruettgar, D., Bateman, R., Groves, D.I., Harris, J.L., Kohler, E.A., 1999. Evidence for diachronous Archean lode gold mineralization in the Yilgarn Craton, Western Australia: a SHRIMP U-Pb study of intrusive rocks. Economic Geology 94, 1259–1276.